HHS Public Access

Author manuscript

Sci Signal. Author manuscript; available in PMC 2017 January 12.

Published in final edited form as:

Sci Signal. ; 9(410): ra5. doi:10.1126/scisignal.aab0467.

Allosteric signaling through an mGlu2 and 5-HT_{2A} heteromeric receptor complex and its potential contribution to schizophrenia

José L. Moreno[1,2], **Patricia Miranda-Azpiazu**[3,4], **Aintzane García-Bea**[2,3,4], **Jason Younkin**[1], **Meng Cui**[1], **Alexey Kozlenkov**[2], **Ariel Ben-Ezra**[2], **Georgios Voloudakis**[2], **Amanda K. Fakira**[5], **Lia Baki**[1], **Yongchao Ge**[6], **Anastasios Georgakopoulos**[2], **José A. Morón**[5,*], **Graeme Milligan**[7], **Juan F. López-Giménez**[7,8], **Nikolaos K. Robakis**[2,9,10], **Diomedes E. Logothetis**[1], **J. Javier Meana**[3,4,11,†], and **Javier González-Maeso**[1,2,6,10,†]

[1]Department of Physiology and Biophysics, Virginia Commonwealth University School of Medicine, Richmond, VA 23298, USA

[2]Department of Psychiatry, Icahn School of Medicine at Mount Sinai, New York, NY 10029, USA

[3]Department of Pharmacology, University of the Basque Country UPV/EHU, E-48940 Leioa, Bizkaia, Spain

[4]Centro de Investigación Biomédica en Red de Salud Mental (CIBERSAM), University of the Basque Country UPV/EHU, E-48940 Leioa, Bizkaia, Spain

[5]Department of Anesthesiology, Columbia University College of Physicians and Surgeons, New York, NY 10032, USA

[6]Department of Neurology, Icahn School of Medicine at Mount Sinai, New York, NY 10029, USA

[7]Molecular Pharmacology Group, Institute of Molecular, Cell and Systems Biology, College of Medical, Veterinary and Life Sciences, University of Glasgow, Glasgow G12 8QQ, Scotland, UK

[8]Instituto de Biomedicina y Biotecnología de Cantabria (IBBTEC-CSIC-UC), E-39011 Santander, Cantabria, Spain

[9]Department of Neuroscience, Icahn School of Medicine at Mount Sinai, New York, NY 10029, USA

[10]Friedman Brain Institute, Icahn School of Medicine at Mount Sinai, New York, NY 10029, USA

[11]BioCruces Health Research Institute, E-48903 Barakaldo, Bizkaia, Spain

†Corresponding author. javier.meana@ehu.eus (J.J.M.); jgmaeso@vcu.edu (J.G.-M.).
*Present address: Department of Anesthesiology, Washington University School of Medicine in St. Louis, St. Louis, MO 63110, USA

Author contributions: J.L.M., J.J.M., and J.G.-M. designed experiments, analyzed data, and wrote the manuscript. J.L.M. performed experiments. J.J.M. supervised the research in postmortem human brain, and obtained and classified postmortem human brain samples. J.G.-M. supervised the research. P.M.A. and A.G.-B. performed assays in mouse and postmortem human brain. J.Y., supervised by D.E.L., performed whole-cell patch-clamp recordings. M.C., supervised by D.E.L., performed molecular modeling. A.K., A.B.-E., and L.B. assisted with experiments. G.V. and A.G., supervised by N.K.R., helped with calcium imaging assays. A.K.F., supervised by J.A.M., helped with subcellular fractionation. Y.G. performed biostatistical analysis. J.F.L.-G., supervised by G.M., performed 3-FRET assays and helped with early calcium imaging studies. All authors discussed the results and commented on the manuscript.

Competing interests: The authors declare that they have no competing interests.

Abstract

Heterotrimeric guanine nucleotide–binding protein (G protein)–coupled receptors (GPCRs) can form multiprotein complexes (heteromers), which can alter the pharmacology and functions of the constituent receptors. Previous findings demonstrated that the $G_{q/11}$-coupled serotonin 5-HT_{2A} receptor and the $G_{i/o}$-coupled metabotropic glutamate 2 (mGlu2) receptor—GPCRs that are involved in signaling alterations associated with psychosis—assemble into a heteromeric complex in the mammalian brain. In single-cell experiments with various mutant versions of the mGlu2 receptor, we showed that stimulation of cells expressing mGlu2–5-HT_{2A} heteromers with an mGlu2 agonist led to activation of $G_{q/11}$ proteins by the 5-HT_{2A} receptors. For this crosstalk to occur, one of the mGlu2 subunits had to couple to $G_{i/o}$ proteins, and we determined the relative location of the $G_{i/o}$-contacting subunit within the mGlu2 homodimer of the heteromeric complex. Additionally, mGlu2-dependent activation of $G_{q/11}$, but not $G_{i/o}$, was reduced in the frontal cortex of 5-HT_{2A} knockout mice and was reduced in the frontal cortex of postmortem brains from schizophrenic patients. These findings offer structural insights into this important target in molecular psychiatry.

Introduction

Heterotrimeric guanine nucleotide–binding protein (G protein)–coupled receptors (GPCRs) represent the largest family of signaling proteins in the mammalian genome, and they are the most common targets for therapeutic drugs (1, 2). These heptahelical transmembrane proteins activate G proteins to modulate cell function (3). G proteins are grouped into four families (G_s, $G_{i/o}$, $G_{q/11}$, and G_{12}) according to the degree of homology of their primary structure and their regulation of specific signaling events. GPCRs have been thought to function as monomers—a model of receptor signaling that is further supported by observations based on assays that measure the agonist binding and G protein coupling of a single purified monomeric family A GPCR, such as the β_2-adrenergic receptor, rhodopsin, and the μ-opioid receptor (4–6). Nevertheless, it is currently widely accepted that the metabotropic glutamate (mGlu) receptors (which are part of the C family of GPCRs) are assembled into strict dimers (7). Similarly, extensive biochemical and biophysical evidence corroborates the existence of homodimers, heterodimers, and oligomers of family A GPCRs that differentially alter receptor–G protein coupling preferences and G protein–dependent signaling (8). Although this model of quaternary interactions is further supported by the increase in studies that have elucidated crystal structures of GPCRs, especially by the dimers found within four of the latest structures (CXCR4, μ-opioid, κ-opioid, and β_1-adrenergic receptors) (9–13), there are a number of open questions about the structural mechanism of crosstalk through dimeric and oligomeric GPCR structures.

Data from studies of mutant α_{1B}-adrenergic receptor–G protein fusions, in which either the G protein or the receptor was specifically deactivated, suggest that GPCRs could operate through an activation mechanism by which the signal would be transmitted from the protomer to which the ligand binds to the neighboring protomer of the homomeric receptor complex (14). A similar mechanism of crosstalk is well documented for the γ-aminobutyric acid B ($GABA_B$) receptor, a family C GPCR. In this case, one subunit ($GABA_B$-R1) binds to the agonist, whereas the other ($GABA_B$-R2) activates the G protein (15, 16). Furthermore,

agonist binding to a single protomer maximally activates a signaling unit consisting of two dopamine D_2 receptors (family A GPCRs) and a single G protein (17); however, results from studies of the family A GPCR leukotriene B4 receptor BLT1 argue against transactivation. These studies demonstrated that, although ligand binding to one protomer in the homodimer is associated with cross-conformational changes, a mechanism of transactivation, in which the ligand-free protomer would trigger the exchange of guanosine 5′-triphosphate (GTP) for guanosine diphosphate (GDP) on the G protein α subunit, could not be considered as a means for G protein activation in this case (18, 19). Much less is known about allosteric communication between components of heteromeric GPCR complexes.

The serotonin 5-HT_{2A} receptor, which is a family A GPCR, and the mGlu2 receptor, which is a family C GPCR, have been linked to the pathophysiology of schizophrenia and other psychotic disorders, as well as to the mechanism of action of atypical antipsychotic drugs (for example, clozapine, olanzapine, and risperidone), and a new class of potential antipsychotic drugs that act as agonists of mGlu2 and mGlu3 receptors (for example, LY379268 and LY404039) (20). These two receptor subtypes are also involved in the molecular mechanism of action of hallucinogenic 5-HT_{2A} receptor agonists, such as lysergic acid diethylamide and psilocin (21). Our previous findings demonstrated that the $G_{q/11}$-coupled 5-HT_{2A} receptor and the $G_{i/o}$-coupled mGlu2 receptor form a specific heteromeric GPCR complex in heterologous expression systems, as well as in mouse and human frontal cortex (22, 23). These data, however, did not address whether 5-HT_{2A} and mGlu2 receptors are expressed as heterodimers or higher-order heteromeric complexes. We also demonstrated that this molecular proximity between 5-HT_{2A} and mGlu2 does not occur with the closely related $G_{i/o}$-coupled mGlu3 receptor, and it is either rescued or disrupted with different mGlu2 or mGlu3 chimeric constructs. Thus, we showed that, acting through the 5-HT_{2A}–mGlu2 receptor heterocomplex, both serotonergic and glutamatergic ligands modulate $G_{q/11}$- and $G_{i/o}$-dependent signaling (24). However, although this pattern of G protein coupling induced by drugs bound to one receptor of the heteromer in the presence of the endogenous ligand of the other receptor (for example, serotonin or glutamate) predicts their propsychotic- and antipsychotic-like behavioral effects (24), the way in which these assemblies function at a molecular level has not been resolved. It is thus unclear whether conformational rearrangements in both protomers of the 5-HT_{2A}–mGlu2 receptor heterocomplex upon ligand binding are necessary for changes in the pattern of G protein coupling.

Here, we focused on the ability of the mGlu2 receptor to activate $G_{q/11}$-dependent signaling through the 5-HT_{2A}–mGlu2 heteromeric complex. The central question was whether agonist binding to the mGlu2 receptor resulted in conformational changes in the other GPCR within the heteromer and, if so, whether conformational changes in both mGlu2 and 5-HT_{2A} receptors were necessary for the activation of $G_{q/11}$ proteins by agonist drugs that bind to the mGlu2 receptor. To that aim, we investigated the effects of the mGlu2 and mGlu3 (mGlu2/3) receptor agonist LY379268 on $G_{q/11}$-dependent signaling in mammalian cells expressing 5-HT_{2A} in the presence or absence of mGlu2, as well as of mGlu2 and mGlu3 chimeric constructs that have different abilities to form 5-HT_{2A}–mGlu2 heteromers. We showed that the presence of both 5-HT_{2A} and mGlu2 in a heteromer was necessary for the stimulation of $G_{q/11}$-dependent signaling by LY379268. We also demonstrated that whereas coexpression

of an mGlu2 receptor with a mutant 5-HT_{2A} receptor defective in G protein activation abolished LY379268-stimulated $G_{q/11}$-dependent signaling, the ability of the mGlu2 receptor to couple to and activate $G_{i/o}$ proteins was required to encode this particular signaling outcome. In addition, our findings define the relative structural orientation of the two mGlu2 protomers within an mGlu2 homodimer that affected 5-HT_{2A} receptor–dependent function, provide evidence for the existence of this signaling crosstalk in mouse frontal cortex, and unravel its functional dysregulation in terms of G protein coupling associated with schizophrenia.

Results

Agonists of mGlu2/3 receptors increase the intracellular Ca^{2+} concentration in HEK 293 cells coexpressing mGlu2 and 5-HT_{2A} receptors

One of the limitations of heterologous expression systems is related to the relative stoichiometry of the receptors and other signaling components that a cell line often does not natively express. Using a *Xenopus* oocyte heterologous expression system, we previously showed that the mGlu2/3 receptor agonist LY379268 cross-signals and elicits $G_{q/11}$-dependent signaling in cells coexpressing 5-HT_{2A} and mGlu2 receptors (24). With the goal of validating these observations in an independent cell line expression system, we quantified G protein–dependent signaling in human embryonic kidney (HEK) 293 cells expressing mGlu2 alone, 5-HT_{2A} alone, or mGlu2 and 5-HT^{2A} together. Stimulation of $G_{q/11}$ elicits a transient increase in the concentration of intracellular calcium ($[Ca^{2+}]_i$) through the inositol 1,4,5-trisphosphate (IP_3)–mediated release of Ca^{2+} from the endoplasmic reticulum, which can be detected with fluorescent calcium-sensitive dyes, such as Fura-2 (25). Cells transfected with equal amounts of plasmids encoding enhanced yellow fluorescent protein (eYFP)–tagged mGlu2 (mGlu2-eYFP), mCherry-tagged 5-HT_{2A} (5-HT_{2A}–mCherry), both mGlu2-eYFP and 5-HT_{2A}–mCherry, or with the empty plasmid pcDNA3.1 were loaded with the Ca^{2+} indicator dye Fura-2 and sequentially exposed to 100 μM LY379268 and 10 μM serotonin. We scored only individual cells that expressed detectable amounts of the respective fluorescent proteins eYFP, mCherry or both. In cells that expressed 5-HT_{2A}–mCherry alone, serotonin, but not the mGlu2/3 agonist LY379268, stimulated an increase in $[Ca^{2+}]_i$ (Fig. 1, A to C). As expected neither serotonin nor LY379268 had such an effect in cells expressing mGlu2-eYFP alone (Fig. 1, A to C). In cells coexpressing mGlu2-eYFP and 5-HT_{2A}–mCherry, LY379268 increased $[Ca^{2+}]_i$ (Fig. 1, A to C). In cells transfected with empty plasmid or plasmid encoding mGlu2-eYFP alone, adenosine 5′-triphosphate (ATP), which activates endogenous $G_{q/11}$-coupled P2Y purinergic receptors (26), resulted in increased $[Ca^{2+}]_i$ (fig. S1). These data suggest that the mGlu2/3 receptor agonist LY379268 induces increases in $[Ca^{2+}]_i$ only in individual HEK 293 cells that coexpress the mGlu2 and 5-HT_{2A} receptors.

To determine whether this functional crosstalk from the mGlu2 receptor that requires the 5-HT_{2A} receptor depends upon the absolute and relative densities of the receptors, we compared the increases in $[Ca^{2+}]_i$ in HEK 293 cells transfected with equivalent amounts of DNA consisting of various ratios of plasmids encoding eYFP- or mCherry-tagged receptors or of empty plasmid (fig. S2, A and B). As was observed earlier (Fig. 1, A to C), LY379268

increased $[Ca^{2+}]_i$ in cells that were transfected with plasmids encoding mGlu2-eYFP and 5-HT_{2A}–mCherry in a 1:1 ratio (Fig. 1D). We observed the largest effect of LY379268 on $[Ca^{2+}]_i$ in cells transfected with plasmids encoding mGlu2-eYFP and 5-HT_{2A}–mCherry in a 1:2 ratio, whereas no increase in $[Ca^{2+}]_i$ was observed in cells transfected with plasmids encoding mGlu2-eYFP and 5-HT_{2A}–mCherry in a 1:3 ratio (Fig. 1D). As expected, a serotonin-dependent increase in $[Ca^{2+}]_i$ was readily detected in cells coexpressing mGlu2-eYFP and 5-HT_{2A}–mCherry, regardless of the ratio of the plasmids used to transfect the cells (Fig. 1D). On the basis of these results, our subsequent assays were performed with HEK 293 cells cotransfected with plasmids encoding mGlu2-eYFP and 5-HT_{2A}–mCherry in a 1:2 ratio.

Previous findings (27), including ours (28), suggested that certain agonists activate some, but not all, of the available signaling pathways, an effect described as “ligand bias.” We tested whether the effect of LY379268 on $[Ca^{2+}]_i$ in HEK 293 cells coexpressing mGlu2-eYFP and 5-HT_{2A}–mCherry was shared by other mGlu2/3 receptor agonists. We assessed the effects of different concentrations of the mGlu2/3 receptor agonists LY379268 and LY404039, as well as that of the endogenous agonist L-glutamate. In individual cells coexpressing mGlu2-eYFP and 5-HT_{2A}–mCherry, all three agonists led to increased $[Ca^{2+}]_i$ (Fig. 1E, left panel, and fig. S3), effects that were prevented by the mGlu2/3 antagonist LY341495 (Fig. 1F). Serotonin stimulated increases in $[Ca^{2+}]_i$ in cells that were cotransfected with plasmids encoding mGlu2-eYFP and 5-HT_{2A}–mCherry (Fig. 1E, right panel, and fig. S3), an outcome that was unaffected by the presence of LY341495 (Fig. 1F).

LY379268 increases $[Ca^{2+}]_i$ through 5-HT_{2A}–mGlu2 heteromers

We previously demonstrated that neither the mGlu3 receptor, which is closely related to the mGlu2 receptor, nor the 5-HT_{2C} receptor, which is closely related to the 5-HT_{2A} receptor, was capable of forming heteromers with the 5-HT_{2A} or mGlu2 receptors, respectively (22). Through experiments with a series of molecular chimeras, we showed that three residues located at the intracellular end of the fourth transmembrane domain (TM4) are necessary for the mGlu2 receptor to be assembled as a GPCR heteromer with the 5-HT_{2A} receptor (23). Thus, substitution of residues Ala-$677^{4.40}$, Ala-$681^{4.44}$, and Ala-$685^{4.48}$ in mGlu2 for Ser-$686^{4.40}$, Phe-$690^{4.44}$, and Gly-$694^{4.48}$ in mGlu3 (to generate the mGlu2ΔTM4N chimera) substantially reduces its ability to form a complex with the 5-HT_{2A} receptor. We also demonstrated previously that an mGlu2/mGlu3 chimera containing TM4 and TM5 of the mGlu2 receptor (mGlu3ΔTM4,5) formed a heteromer with the 5-HT_{2A} receptor (22).

To test whether the Ca^{2+} signal induced by activation of the mGlu2 receptor in cells coexpressing the mGlu2 and 5-HT_{2A} receptors required heteromer formation, we monitored LY379268-stimulated $[Ca^{2+}]_i$ signaling in HEK 293 cells cotransfected with plasmids encoding 5-HT_{2A}–mCherry and mGlu2-eYFP, mGlu3-eYFP, mGlu2ΔTM4N-eYFP, or mGlu3ΔTM4,5-eYFP. LY379268 stimulated $[Ca^{2+}]_i$ release in cells co-expressing the mGlu2-eYFP receptor and the 5-HT_{2A}–mCherry receptor (Fig. 1G). In contrast, LY379268 did not stimulate $[Ca^{2+}]_i$ release in cells coexpressing mGlu3-eYFP and 5-HT_{2A}–mCherry (Fig. 1G) or in cells coexpressing mGlu2-eYFP and a C-terminally c-Myc–tagged 5-HT_{2C} receptor (fig. S4). The signaling response to the mGlu2/3 agonist was absent in cells

coexpressing 5-HT_{2A}–mCherry and mGlu2ΔTM4N-eYFP but was rescued in cells coexpressing 5-HT_{2A}–mCherry and mGlu3ΔTM4,5-eYFP (Fig. 1G). Each of these chimeric constructs was expressed at the plasma membrane (fig. S5), and we determined previously by [^{3}H]LY341495 binding saturation curves that their relative abundances are comparable (22, 23). Similarly, when expressed as homodimers, each of the mGlu2/mGlu3 chimera constructs facilitated $G_{i/o}$-dependent signaling (Fig. 1H). Thus, the potency and efficacy of LY379268-stimulated [^{35}S]GTPγS binding were similar in plasma membrane preparations of cells transfected with either mGlu2-eYFP, mGlu3-eYFP, mGlu2ΔTM4N-eYFP, or mGlu3Δ-TM4,5-eYFP, ($F_{9,68}$ = 1.65, P > 0.05) (Fig. 1H). Together, these findings suggest that activation of the mGlu2 receptor stimulates increased $[Ca^{2+}]_i$ through a molecular mechanism that requires the presence of both the mGlu2 and 5-HT_{2A} receptors in a heteromeric complex.

A 5-HT_{2A} receptor that activates G proteins is necessary for the increased $[Ca^{2+}]_i$ caused by agonist binding to the mGlu2 receptor in 5-HT_{2A}–mGlu2 heteromers

We tested whether functional coupling of the 5-HT_{2A} receptor to G proteins was required for signaling crosstalk between the components of the 5-HT_{2A}–mGlu2 receptor heterocomplex. Addition of the 5-HT_{2A} receptor inverse agonist M100,907 (volinanserin) blocked the effect of both LY379268 and serotonin on Ca^{2+} release in cells coexpressing mGlu2-eYFP and 5-HT_{2A}–mCherry (Fig. 2A). As expected, however, the ability of ATP to induce an increase in the $[Ca^{2+}]_i$ concentration was unaffected by M100,907 in cells coexpressing mGlu2-eYFP and 5-HT_{2A}–mCherry (fig. S1B).

Considering that inverse agonists stabilize an inactivated state of the receptor (24), we next tested whether 5-HT_{2A} receptor–dependent function was involved in the crosstalk mechanism between the components of the 5-HT_{2A}–mGlu2 heterocomplex. Previous findings demonstrated that mutation of a conserved hydrophobic leucine or isoleucine in intracellular loop 2 (ICL2) of the $G_{q/11}$-coupled α_{1B}-adrenergic and histamine H_1 receptors eliminates agonist-mediated signaling but not agonist binding (14). Thus, we substituted Ile^{181} in the 5-HT_{2A} receptor for aspartate (an I181D mutation). We found that this mutation in ICL2 eliminated the serotonin-stimulated increase in $[Ca^{2+}]_i$ concentration in cells expressing 5-HT_{2A}–I181D–mCherry (Fig. 2B). Furthermore, despite 5-HT_{2A}–I181D–mCherry and mGlu2-eYFP being in close proximity to each other as determined by flow cytometric analysis of fluorescence resonance energy transfer (FCM-based FRET; fig. S6, A and B), LY379268 did not stimulate increased $[Ca^{2+}]_i$ (Fig. 2B). Thus, no signaling crosstalk was observed between mGlu2 and a 5-HT_{2A} receptor carrying a mutation that abolishes 5-HT_{2A}–dependent G protein activation. ATP induced Ca^{2+} release in cells coexpressing 5-HT_{2A}–I181D–mCherry and mGlu2-eYFP (fig. S1C). 5-HT_{2A} and 5-HT_{2A}–I181D showed equivalent plasma membrane expression and densities as defined by immunocytochemical assays (fig. S5A) and [^{3}H]ketanserin binding saturation curves in plasma membrane preparations (fig. S7A), respectively. Together with the effects of M100,907 on LY379268-dependent Ca^{2+} release (Fig. 2A), these findings suggest that a 5-HT_{2A} receptor that interacts with G proteins is required for the effects of the mGlu2/3 receptor agonist LY379268 on $[Ca^{2+}]_i$ signaling in cells expressing 5-HT_{2A}–mGlu2 heteromers.

Previous findings suggested that under certain conditions, GPCRs whose canonical signaling pathway is mediated by $G_{i/o}$ may also activate phospholipase C (PLC), the first signaling component downstream of $G_{q/11}$ in most experimental systems (29, 30). To test whether activation of $G_{q/11}$-dependent signaling was of central importance for the effects of the mGlu2/3 receptor agonist LY379268 in cells coexpressing 5-HT_{2A} and mGlu2 receptors, we measured the ability of the selective $G_{q/11}$ inhibitor UBO-QIC (also known as FR900359) to prevent increased $[Ca^{2+}]_i$ mobilization (31). We found that the effect of LY379268 on Ca^{2+} release in cells coexpressing mGlu2-eYFP and 5-HT_{2A}–mCherry was abolished in the presence of UBO-QIC (Fig. 2C). The serotonin-stimulated increase in $[Ca^{2+}]_i$ was also disrupted by UBO-QIC in cells coexpressing 5-HT_{2A}–mCherry and mGlu2-eYFP (Fig. 2C). As expected, this inhibitor of $G_{q/11}$-dependent signaling also blocked the ATP-stimulated increase in $[Ca^{2+}]_i$ in control-transfected cells (fig. S1D). The PLC-γ inhibitor U73122 disrupted both LY379268-and serotonin-dependent Ca^{2+} release (Fig. 2D). U73122 also blocked the ATP-stimulated increase in $[Ca^{2+}]_i$ in control-transfected cells (fig. S1E). Together, these results corroborate the idea that the effect of the mGlu2/3 agonist LY379268 on Ca^{2+} release in cells coexpressing 5-HT_{2A} and mGlu2 heteromers is $G_{q/11}$-dependent.

An mGlu2 receptor that activates G proteins is necessary for the increase in $[Ca^{2+}]_i$ induced by agonist binding to mGlu2 through the 5-HT_{2A}–mGlu2 heterocomplex

To further clarify how agonist binding to the mGlu2 component of the 5-HT_{2A}–mGlu2 heteromer led to Ca^{2+} signaling, we introduced the F756S mutation into the ICL3 of mGlu2, which abolishes G protein activation (32). We first confirmed that the plasma membrane abundance (fig. S5A) and binding properties of mGlu2-F756S (fig. S7B) were unaffected. Our data also showed that mGlu2-F756S–eYFP and 5-HT_{2A}–mCherry were found in close proximity to each other (fig. S6, C and D). However, LY379268 did not induce Ca^{2+} release in cells coexpressing mGlu2-F756S–eYFP and 5-HT_{2A}–mCherry (Fig. 2E). Serotonin induced an increase in $[Ca^{2+}]_i$ in cells coexpressing mGlu2-F756S–eYFP and 5-HT_{2A}–mCherry (Fig. 2E). These data suggest that an mGlu2 receptor that can activate $G_{i/o}$ proteins is necessary for the LY379268-mediated increase in $[Ca^{2+}]_i$. An alternative, although not mutually exclusive, explanation of these results is that mGlu2-F756S affects the conformational properties (and hence the signaling) of the 5-HT_{2A}–mGlu2 heteromer through a mechanism that does not require the activation of $G_{i/o}$ proteins. To directly examine whether coupling to $G_{i/o}$ was necessary for the effect of LY379268 on Ca^{2+} release in cells expressing mGlu2 and 5-HT_{2A} heteromers, we investigated the effect of pertussis toxin (PTX), which induces the adenosine diphosphate (ADP) ribosylation of the α subunit of heterotrimeric $G_{i/o}$ proteins, locking the α subunit into a GDP-bound inactive state; thus, PTX can disrupt the function of both the α and βγ subunits of $G_{i/o}$ proteins. LY379268 failed to increase $[Ca^{2+}]_i$ in PTX-treated HEK 293 cells coexpressing mGlu2-eYFP and 5-HT_{2A}–mCherry (Fig. 2F), a result that differs from that previously obtained from experiments with oocytes (24). As expected, PTX did not affect serotonin-induced Ca^{2+} release in cells coexpressing 5-HT_{2A}–mCherry and mGlu2-eYFP (Fig. 2F). Together with our findings from experiments with mGlu2-F756S, these results suggest that coupling to and activation of $G_{i/o}$ proteins is necessary for the 5-HT_{2A}–mGlu2 heteromer–dependent effects of the mGlu2/3 agonist LY379268.

The effects of LY379268 on Ca^{2+} release in cells expressing the 5-HT_{2A}–mGlu2 heterocomplex depend on $G\alpha_{i/o}$ but not on $G\beta\gamma$

To gain insight into the crosstalk mechanism between the mGlu2 and 5-HT_{2A} receptors, we directly compared the effects of NF023, which selectively inhibits the α subunit of $G_{i/o}$ proteins (33), with those of a Gβγ-blocking peptide (MPS phosducin-like protein C-terminus) (34). LY379268 did not induce Ca^{2+} release in cells coexpressing mGlu2-eYFP and 5-HT_{2A}–mCherry in the presence of NF023 (Fig. 2G). On the contrary, MPS had no effect on the LY379268-dependent increase in $[Ca^{2+}]_i$ in cells coexpressing mGlu2-eYFP and 5-HT_{2A}–mCherry (Fig. 2H). Neither NF023 nor MPS disrupted serotonin-stimulated Ca^{2+} release in cells expressing both 5-HT_{2A}–mCherry and mGlu2-eYFP (Fig. 2, G and H). As an internal control, we next asked whether MPS disrupted Gβγ-dependent activity in HEK 293 cells. GIRK channels are sensitive to the Gβγ subunits of $G_{i/o}$ proteins (35). As expected, the presence in HEK 293 cells of the nonhydrolyzable GTP analog GTPγS, which induces the constitutive activation of heterotrimeric G proteins, led to stimulation of GIRK currents (Fig. 2, I and J). This effect of GTPγS on Gβγ-dependent activity was prevented in the presence of the Gβγ-blocking peptide MPS (Fig. 2, I and J). These findings demonstrate that whereas the Gβγ-blocking peptide MPS has repressive effects on Gβγ-dependent channel activity in HEK 293 cells, the presence of MPS did not affect the impact of LY379268 on Ca^{2+} release in cells coexpressing mGlu2-eYFP and 5-HT_{2A}–mCherry.

A functionally active mGlu2 homodimer rescues the increased $[Ca^{2+}]_i$ induced by LY379268 through the 5-HT_{2A}–mGlu2 heterocomplex

To explore further the specific role of the mGlu2 component in the effect on Ca^{2+} release, we tested any possible functional complementation between two nonfunctional mGlu2 protomers and the 5-HT_{2A} receptor (Fig. 2, K and L). We combined the use of bimolecular fluorescence complementation (BiFC) (36) and mGlu2 constructs carrying mutations in lobe II of the Venus flytrap domain (Y216A, D295A; YADA) (37), which abolished ligand binding (fig. S7B) and receptor function (Fig. 2L), without disrupting plasma membrane expression (fig. S5A), or mutations in ICL3 (F756S), which abolished G protein activation (Fig. 2L). We first validated that the effect of LY379268 on increased $[Ca^{2+}]_i$ was absent in cells coexpressing Y216A-D295A–mGlu2-eYFP (YADA-mGlu2-eYFP) and 5-HT_{2A}–mCherry (Fig. 2K), even though both constructs were found in close proximity to each other, as defined by FCM-based FRET (fig. S6, C and D). Similarly, and as expected on the basis of previous findings that showed that mGlu2 receptors form stable homodimers (38), BiFC was observed in cells coexpressing mGlu2 with either the N-terminal 172–amino acid fragment or the C-terminal 67–amino acid fragment of mCitrine (mCi-N172 and mCi-C67, respectively) (fig. S5, B and C). We also confirmed that the mGlu2/3 agonist LY379268 stimulated $G_{i/o}$-dependent signaling in cells coexpressing YADA–mGlu2–mCi-N172 and mGlu2-F756S–mCi-C67 (Fig. 2L). Thus, linear versus nonlinear regression analysis showed that LY379268-stimulated [^{35}S]GTPγS binding in cells expressing mGlu2-eYFP could be fit preferentially by a concentration-response curve, whereas linear regression analysis provided the best fit to LY379268-stimulated [^{35}S]GTPγS binding in cells expressing either YADA-mGlu2-eYFP alone or mGlu2-F756S–eYFP alone, as assessed by *F* test (Fig. 2L). Linear versus nonlinear regression analysis showed that LY379268-stimulated [^{35}S]GTPγS binding in cells coexpressing YADA–mGlu2–mCi-N172 and mGlu2-F756S–mCi-C67 can

be fit preferentially by a concentration-response curve, as assessed by *F* test (Fig. 2L). Additionally, the potency and efficacy of LY379268 stimulating [^{35}S]GTPγS binding were similar in plasma membrane preparations of cells expressing mGlu2-eYFP or coexpressing YADA–mGlu2–mCi-N172 and mGlu2-F756S–mCi-C67 ($F_{3,46}$ = 0.40, P > 0.05) (Fig. 2E). Note that the effect of LY379268 on Ca^{2+} release was rescued in cells coexpressing YADA–mGlu2–mCi-N172 and mGlu2-F756S–mCi-C67 together with 5-HT_{2A}–mCherry (Fig. 2K). Serotonin induced increases in $[Ca^{2+}]_i$ in cells coexpressing 5-HT_{2A}–mCherry with mGlu2-eYFP, YADA-mGlu2-eYFP, or YADA–mGlu2–mCi-N172 and mGlu2-F756S–mCi-C67 but not in control-transfected cells (Fig. 2K). These findings suggest that a fully functional mGlu2 homodimeric receptor complex and its intrinsic G protein coupling properties are fundamental for this component of the 5-HT_{2A}–mGlu2 heteromeric receptor complex to crosstalk with the 5-HT_{2A} component.

Characterization of the relative orientation of the two mGlu2 protomers that affect 5-HT_{2A} receptor–dependent function

The data thus far suggest that the expression of an mGlu2 mutant receptor that binds to orthosteric agonists (that is, an agonist that binds to the same binding site on the GPCR as the endogenous agonist), but does not activate G proteins, together with an mGlu2 mutant that does not bind to ligands, but retains intact the regions involved in G protein coupling, rescues the $G_{q/11}$-dependent signaling events induced by the mGlu2/3 agonist LY379268 through the 5-HT_{2A}–mGlu2 heteromer. These results, together with our previous demonstration that the intracellular end of TM4 of mGlu2 is necessary to form a protein complex with the 5-HT_{2A} receptor (23), led us to explore the relative location of the mGlu2 protomer that needs to make contact with $G_{i/o}$ to enable crosstalk with 5-HT_{2A} receptor. We attempted to answer this question by combining mGlu2/mGlu3 chimeric constructs that disrupt 5-HT_{2A}–mGlu2 heteromer formation with mutations in either the Venus flytrap module or the ICL3 of the mGlu2 receptor, which specifically affect ligand binding or G protein coupling, respectively. We hypothesized that if the mGlu2 protomer that directly makes contact with the 5-HT_{2A} receptor is fundamental for interacting with $G_{i/o}$ proteins, then the effect of the mGlu2/3 agonist LY379268 on Ca^{2+} release through the 5-HT_{2A}–mGlu2 heteromer would be disrupted in cells coexpressing YADA–mGlu2ΔTM4N–mCi-N172 (an mGlu2 mutant that cannot bind to orthosteric agonists or form 5-HT_{2A}–mGlu2 heteromers) and mGlu2-F756S–mCi-C67 (an mGlu2 mutant that does not activate $G_{i/o}$ proteins) together with 5-HT_{2A}–mCherry (Fig. 3A). Alternatively, if the distal mGlu2 protomer is necessary for $G_{i/o}$ protein coupling, then the effect of the mGlu2/3 agonist LY379268 on Ca^{2+} release stimulated by 5-HT_{2A}–mGlu2 heteromers would be disrupted in cells coexpressing YADA–mGlu2–mCi-N172 (an mGlu2 mutant that cannot bind to orthosteric agonists) and mGlu2ΔTM4N-F756S–mCi-C67 (an mGlu2 mutant that cannot activate $G_{i/o}$ proteins or form 5-HT_{2A}–mGlu2 heteromers) together with 5-HT_{2A}–mCherry (Fig. 3B). We found that LY379268 induced Ca^{2+} release in cells coexpressing YADA–mGlu2ΔTM4N–mCi-N172 and mGlu2-F756S–mCi-C67 with 5-HT_{2A}–mCherry (Fig. 3, A and C), but not in cells coexpressing YADA–mGlu2–mCi-N172 and mGlu2ΔTM4N-F756S–mCi-C67 with 5-HT_{2A}–mCherry (Fig. 3, B and C).

Additional controls included plasma membrane expression (figs. S5, B and C, and S7B) and the presence of G protein coupling in cells coexpressing either YADA–mGlu2ΔTM4N–mCi-N172 and mGlu2-F756S–mCi-C67 or YADA–mGlu2–mCi-N172 and mGlu2ΔTM4N-F756S–mCi-C67 constructs (Fig. 3D). Thus, the potency and efficacy of LY379268 stimulating [^{35}S]GTPγS binding were similar in plasma membrane preparations of cells cotransfected with YADA–mGlu2ΔTM4N–mCi-N172 and mGlu2-F756S–mCi-C67 as compared to those obtained in cells co-transfected with YADA–mGlu2–mCi-N172 and mGlu2ΔTM4N-F756S–mCi-C67 ($F_{3,130}$ = 0.49, P > 0.05) (Fig. 3D). These data suggest that the mGlu2 promoter that binds to LY379268 must have an intact TM4 with which to communicate with 5-HT$_{2A}$. The data also suggest that $G_{i/o}$ protein coupling to the distal mGlu2 protomer within the 5-HT$_{2A}$–mGlu2 heteromeric receptor complex is necessary to induce Ca^{2+} release through $G_{q/11}$ proteins.

Computational modeling and experimental evidence reveal higher-order oligomerization

Previous studies suggested that family A GPCRs form homodimers or higher-order oligomers in live cells (8). Thus, we tested whether at least two 5-HT$_{2A}$ receptor molecules formed part of the 5-HT$_{2A}$–mGlu2 heteromeric complex. We established in our experimental system the conditions to monitor sequential 3-FRET and used this biophysical approach to detect oligomeric complexes in single live cells. Three fluorescent proteins(Cerulean, mCitrine, and mCherry) were selected on the basis of the overlaps of the emission wavelengths of the donors with the excitation of wavelengths of the acceptors (see Materials and Methods). Additional assays were performed with the nonfluorescent variant of mCitrine (Y^{67}C). The incorporation of an N-terminal c-Myc epitope tag into the construct enabled the immunological detection of 5-HT$_{2A}$–mCitrine-Y^{67}C and showed that it had the same pattern of distribution as did 5-HT$_{2A}$–mCitrine (fig. S8). Coexpression of 5-HT$_{2A}$–Cerulean, 5-HT$_{2A}$–mCitrine, and mGlu2-Cherry followed by excitation at 425 nm resulted in FRET between Cerulean and mCherry (Fig. 4A) and between Cerulean and mCitrine (Fig. 4B). Excitation of cells with 495-nm light resulted in FRET between mCitrine and mCherry (Fig. 4C). When 5-HT$_{2A}$–Cerulean, 5-HT$_{2A}$–mCitrine-Y^{67}C, and mGlu2-mCherry were expressed together, the FRET between Citrine and mCherry was almost eliminated (Fig. 4A). Because FRET signals were normalized to take into account any variation in the abundances of the different constructs (see Materials and Methods), this suggests that the difference in the FRET signal between Cerulean and mCherry in live cells coexpressing 5-HT$_{2A}$–Cerulean, 5-HT$_{2A}$–mCitrine, and mGlu2-Cherry compared to that observed in cells coexpressing 5-HT$_{2A}$–Cerulean, 5-HT$_{2A}$–mCitrine-Y^{67}C, and mGlu2-mCher-ry likely corresponds to sequential FRET signal from Cerulean to mCitrine and then to mCherry. Together, these studies suggest that at least a portion of these receptors in cells were within an oligomeric complex in which the components were at distances that enabled FRET.

We next focused our attention on the relative location of the 5-HT$_{2A}$ receptor molecules within the 5-HT$_{2A}$–mGlu2 heteromeric complex. Much evidence indicates that TM1 and TM4 contribute to symmetrical interfaces in homomeric complexes of family A GPCRs (8). As discussed earlier, we previously identified that TM4 of the mGlu2 receptor is necessary for it to form heteromers with the 5-HT$_{2A}$ receptor (23). With the goal of defining the TM domains of 5-HT$_{2A}$ that are responsible for the formation of 5-HT$_{2A}$–mGlu2 heteromers, we

performed immunoprecipitation assays with antibodies against the c-Myc tag in plasma membrane preparations of HEK 293 cells transfected with plasmid encoding the hemagglutinin (HA)–tagged form of the mGlu2 receptor alone or together with plasmid encoding a c-Myc–tagged form of the 5-HT_{2A} receptor or an equivalent c-Myc–tagged 5-HT_{2A}/5-HT_{2C} receptor chimera (Fig. 4, D and E). Similar to a previous report (23), when lysates of cells coexpressing HA-mGlu2 and c-Myc–5-HT_{2A} were subjected to immunoprecipitation with anti–c-Myc antibodies, we observed coimmunoprecipitation of a band that was detectable with an anti-HA antibody, which did not occur when coimmunoprecipitations were performed with cells expressing either HA-mGlu2 or c-Myc–5-HT_{2A} alone or when plasma membrane preparations from cells expressing either the HA- or the c-Myc–tagged forms of the receptors were combined before immunoprecipitation was performed (Fig. 4D). Furthermore, immunodetection of an HA-containing protein was not observed when lysates of cells coexpressing 5-HT_{2C}–c-Myc and HA-mGlu2 were subjected to immunoprecipitation with anti–c-Myc antibody (Fig. 4D). Such observations are consistent with the formation of receptor complexes between the tagged forms of mGlu2 and 5-HT_{2A} receptors but not 5-HT_{2C} receptors.

The differences in the capacity of the 5-HT_{2A} and 5-HT_{2C} receptors to interact with the mGlu2 (see also fig. S4) and their close sequence similarity provided the basis for identifying the specific regions of the 5-HT_{2A} receptor that were responsible for the formation of 5-HT_{2A}–mGlu2 heteromers. A study of molecular chimeras of 5-HT_{2A} and 5-HT_{2C} receptors demonstrated that TM4, but not TM1, of the 5-HT_{2A} receptor was necessary for the formation of a complex with the mGlu2 receptor (Fig. 4E and fig. S5D). Together with our earlier 3-FRET data that revealed higher-order heteromerization (Fig. 4, A to C) and our findings focused on functional complementation between two nonfunctional mGlu2 protomers (Fig. 3), these results suggest that the mGlu2 protomer located distally from the 5-HT_{2A} homomer within the 5-HT_{2A}–mGlu2 heteromer was necessary to activate $G_{i/o}$ proteins, which consequently led to the transactivation of 5-HT_{2A}. We built a homology model of the 5-HT_{2A}–mGlu2 heteromer (see Materials and Methods) together with $G_{i/o}$ and $G_{q/11}$ proteins that is consistent with our experimental results (Fig. 5).

$G_{q/11}$-dependent signaling in response to the activation of mGlu2 requires the presence of 5-HT_{2A} receptors in the mouse frontal cortex

A key question in validating the biological relevance of GPCR heteromeric complexes is whether this structural arrangement exists and functions in native tissue. Our previous work demonstrated that immunoprecipitation experiments performed with anti–5-HT_{2A} antibodies and plasma membrane preparations of mouse frontal cortex results in coimmunoprecipitation of anti-mGlu2 immunoreactivity (23). Nevertheless, it is unclear whether 5-HT_{2A} and mGlu2 receptors form part of the same protein complex in presynaptic or postsynaptic cortical membranes. To study the potential contribution of presynaptic and postsynaptic 5-HT_{2A} and mGlu2 receptors to signaling crosstalk, we performed sub-cellular fractionations to purify fractions enriched in presynaptic active zone (PAZ) and postsynaptic density (PSD) proteins. We confirmed the enrichment of PSD proteins (PSD-95) and the absence of detectable PAZ proteins (syntaxin-1) in the PSD fraction, as well as the absence of detectable PSD proteins and the enrichment of PAZ proteins in the PAZ fraction of the

mouse frontal cortex (Fig. 6A). Furthermore, 5-HT_{2A} was detected only in the PSD, whereas mGlu2 was detected in both the PSD and PAZ fractions (Fig. 6B). Together with our previous findings showing coimmunoprecipitation of cortical 5-HT_{2A} and mGlu2 receptors (24), these data suggest that 5-HT_{2A} and mGlu2 may form a protein complex at the PSD in the mouse frontal cortex.

To further explore whether 5-HT_{2A} and mGlu2 receptors exhibited crosstalk and affected G protein coupling in native tissue, we performed [^{35}S]GTPγS binding assays followed by immunoprecipitation with antibodies against $G\alpha_{i1,2,3}$ proteins or $G\alpha_{q/11}$ proteins in plasma membrane preparations from the mouse frontal cortex. Activation of $G\alpha_{i1,2,3}$ and $G\alpha_{q/11}$ was markedly induced by LY379268 in the frontal cortex of wild-type mice (Fig. 6, C to F), effects that were reduced in the presence of the mGlu2/3 receptor antagonist LY341495 (Fig. 6, C to F). We also found that the ability of LY379268 to activate $G_{i1,2,3}$ and $G\alpha_{q/11}$ was absent in the frontal cortex of *mGlu2*$^{-/-}$ mice (Fig. 6, C and D). Further-more, when the coupling of mGlu2 to G proteins was tested in frontal cortex of *5HT2A*$^{-/-}$ mice, LY379268 stimulated the activation of $G_{i1,2,3}$ proteins (Fig. 6E), but the LY379268-dependent activation of $G_{q/11}$ proteins was substantially reduced (Fig. 6F). These data suggest that the canonical coupling of mGlu2 receptors to $G_{i1,2,3}$ proteins is unaffected by the loss of the 5-HT_{2A} receptor but that its coupling to $G_{q/11}$ proteins requires the presence of the 5-HT_{2A} receptor in the mouse frontal cortex.

Alterations in G protein coupling through 5-HT_{2A}–mGlu2 heteromers in postmortem frontal cortex tissue from schizophrenic subjects

A previous study suggested that drugs that activate the mGlu2 receptor may represent an approach to treat schizophrenia (39). We previously found that the density of 5-HT_{2A} receptors in the frontal cortex of postmortem schizophrenic subjects, as defined by [^{3}H]ketanserin binding saturation curves, is increased compared to that in the frontal cortex of normal subjects, whereas the density of the mGlu2 receptor, as defined by [^{3}H]LY341495 binding saturation curves and quantitative real-time polymerase chain reaction (PCR) assays, is reduced, a pattern that could predispose patients to psychosis (22, 23, 40, 41). Here, we investigated in postmortem frontal cortex samples of schizophrenic subjects and individually matched controls (table S1) the pattern of G protein coupling that, on the basis of our findings in heterologous expression systems and mouse frontal cortex, requires expression of 5-HT_{2A} and mGlu2 heteromers. We performed [^{35}S]GTPγS binding assays followed by immunoprecipitation with antibodies against $G\alpha_{i1,2,3}$ or $G\alpha_{q/11}$. Activation of $G\alpha_{i1,2,3}$ proteins was markedly induced by LY379268 in plasma membrane preparations of postmortem human frontal cortex in a concentration-dependent manner (Fig. 7A). Furthermore, the extent of activation of $G_{q/11}$ proteins by LY379268 was substantially reduced in frontal cortex preparations from schizophrenic subjects compared to that in the frontal cortex of controls (Fig. 7B), whereas the LY379268-dependent activation of $G\alpha_{i1,2,3}$ proteins was unaffected (Fig. 7A and table S2). The ability of LY379268 to activate $G\alpha_{i1,2,3}$ and $G\alpha_{q/11}$ proteins was reduced by the mGlu2/3 receptor antagonist LY341495 (Fig. 7, A and B).

Discussion

Previous studies provided mechanistic insights into functional complementation between protomers of family A and family C GPCRs in homomeric and homodimeric complexes, including the homomeric α_{1B}-adrenoreceptor (26), the homomeric dopamine D_2 receptor (17), and the homodimeric mGlu1 receptor (37, 42). However, whereas functional analysis has demonstrated that GPCR heteromers behave differently both in heterologous expression systems and in animal models as compared to GPCR homomers (8), understanding the precise structural determinants underlying how individual protomers within a GPCR heteromeric complex crosstalk with each other has been a major biochemical challenge. We previously showed that the $G_{q/11}$-coupled 5-HT_{2A} receptor and the $G_{i/o}$-coupled mGlu2 receptor form a GPCR heteromer through which ligands that bind to the 5-HT_{2A} receptor modulate $G_{i/o}$-dependent signaling, whereas ligands that bind to the mGlu2 receptor modulate $G_{q/11}$-dependent signaling (22, 24). Here, we reported on the crosstalk mechanism between the components of the 5-HT_{2A}–mGlu2 heteromer. Through an experimental approach to dissect the various components that contribute to the response induced by activation of the 5-HT_{2A}–mGlu2 heteromer, we showed that functional coupling of the mGlu2 receptor to $G_{i/o}$ proteins was necessary for mGlu2/3 receptor agonists to crosstalk through the heteromeric receptor complex, consequently stimulating $G_{q/11}$-dependent signaling. We also delineated the relative location of the mGlu2 protomer within the mGlu2 homodimer that needs to couple to $G_{i/o}$ proteins to transactivate the 5-HT_{2A} receptor. Because some of these findings were validated in mouse and human frontal cortex, the proposed mechanistic explanation for crosstalk between the 5-HT_{2A} and mGlu2 receptors may be generalizable to other experimental systems and to native tissues. The translational potential of these results is substantiated by our findings that the activation of $G_{q/11}$ signaling by the mGlu2/3 agonist LY379268 was dysregulated in the postmortem frontal cortex of schizophrenic subjects.

A key conclusion drawn from our experiments with mGlu2 receptors with mutations in ICL3 and the blockade of $G_{i/o}$ protein coupling by PTX is that functional coupling to $G_{i/o}$ proteins was necessary for drugs that activate the mGlu2 receptor to stimulate increased $[Ca^{2+}]_i$ concentrations in cells coexpressing 5-HT_{2A} and mGlu2 receptors. Previous findings in live cells are consistent with the hypothesis that, for certain GPCR systems, the minimal signaling unit necessary to activate a single G protein is composed of at least two GPCR protomers (17, 37). Additionally, a study based on the generation of nanodiscs containing either one or two GPCR molecules indicates that only a single protomer interacts with the G protein (43). Our data further extend these findings and suggest that the coupling of the mGlu2 receptor to $G_{i/o}$ proteins is necessary for drugs that activate mGlu2 to elicit $G_{q/11}$-dependent signaling when this glutamate receptor is in close proximity to the 5-HT_{2A} receptor. This effect of agonist activation of mGlu2 on increases in the concentration of $[Ca^{2+}]_i$ in cells expressing mGlu2 and 5-HT_{2A} heteromers also demonstrates that the binding of orthosteric agonists to the $G_{i/o}$-coupled mGlu2 receptor initiates structural rearrangements that are consequently transmitted to the $G_{q/11}$-coupled 5-HT_{2A} receptor. Thus, our findings showed that either a single point mutation in ICL2 of the 5-HT_{2A} receptor, which disrupts receptor–G protein coupling without having major effects on the proximity between the 5-

HT_{2A} and mGlu2 receptors, or the selective $G_{q/11}$ inhibitor UBO-QIC abolishes the ability of mGlu2 to elicit calcium signaling in response to LY379268 through the 5-HT_{2A}–mGlu2 heteromer. Further experiments analyzing single 5-HT_{2A}–mGlu2 heteromers will be needed to shed light on whether $G_{i/o}$ and $G_{q/11}$ proteins simultaneously or sequentially couple to the GPCR heteromer. To achieve this, it will be crucial to incorporate knowledge gained from crystallographic studies that have provided convincing evidence that the TM7 domain of mGlu1 forms a parallel homodimer with an interface mediated mainly through TM1 (44), as well as from in vitro assays focused on the dynamics of the mGlu2 homodimeric interface during receptor activation (45).

Although homodimerization is a requirement for the ability of mGlu receptors to couple to and activate G proteins in live cells (37), the exact location of the mGlu2 protomer within the 5-HT_{2A}–mGlu2 heteromer that needs to contact the $G_{i/o}$ protein to crosstalk with the 5-HT_{2A} receptor was unclear. Here, we took advantage of the trans-protomer allosteric regulation between mGlu2 and 5-HT_{2A} to determine to which of the two mGlu2 protomers the $G_{i/o}$ heterotrimer could be docked. We measured the effect of the mGlu2/3 receptor agonist LY379268 on Ca^{2+} release in HEK 293 expressing two mutant mGlu2 protomers, one of which binds to orthosteric agonists but cannot activate G proteins, whereas the other cannot bind to orthosteric agonists but can still interact with G proteins and the 5-HT_{2A} receptor. Although previous computer modeling studies proposed the relative location of the heterotrimeric G protein with respect to a higher-order family A GPCR homomer (9), our findings provide insights into the structural mechanism underlying G protein coupling crosstalk between the components of the 5-HT_{2A}–mGlu2 heteromer. Thus, these data suggest that the coupling of $G_{i/o}$ to the distal mGlu2 protomer is required for the activation of $G_{q/11}$-dependent signaling by mGlu2/3 agonists through the receptor heteromer in live cells.

We and others have confirmed in HEK 293 cells that at least a fraction of the populations of mGlu2 and 5-HT_{2A} receptors constitute part of the same protein complex, as defined by coimmunoprecipitation assays (23, 46). Furthermore, both receptors are found in close proximity to each other as defined independently by biophysical assays such as BRET (bioluminescence resonance energy transfer) (22), FRET (23), antibody-based time-resolved FRET (TR-FRET) (46), and a combination of TR-FRET and the SNAP-tag approach (47). Previous data demonstrated that functional crosstalk between particular subtypes of $G_{i/o}$- and $G_{q/11}$-coupled receptors does not require both receptors to be proximal to each other (46). Thus, it was reported that activation of the $G_{i/o}$-coupled $GABA_B$ receptor enhances the mGlu1 receptor–mediated activation of $G_{q/11}$ proteins through a mechanism that does not require any physical interaction between the $GABA_B$ and mGlu1 receptors (46). It was also established that this crosstalk between $GABA_B$ and mGlu1 receptors is mediated through the $G\beta\gamma$ subunit of the $G_{i/o}$ proteins that couple to the $GABA_B$ receptor (46). Through experiments with wild-type 5-HT_{2C} and mGlu3 receptors, as well as with mGlu2/mGlu3 chimeric constructs that differed in their ability to form heteromers with 5-HT_{2A}, our previous and current results provide evidence for the existence of a crosstalk mechanism between these two receptors that requires their physical association (22–24). Additionally, our findings suggest that $G\alpha_{i/o}$, but not the $G\beta\gamma$ subunit of $G_{i/o}$ proteins released after activation of the mGlu2 receptor, is necessary for the crosstalk between mGlu2 and the

$G_{q/11}$-coupled 5-HT_{2A} receptor. This represents an alternative crosstalk mechanism between coexpressed receptors that are coupled to different G proteins, which is supported by findings demonstrating that agonist alone does not fully stabilize the active conformation of the β_2-adrenergic receptor (48). Further work is needed to define the biophysical and cellular trafficking processes that modulate heteromeric assembly of the 5-HT_{2A} and mGlu2 receptors and how these events, as well as signaling crosstalk and com-partmentalization in membrane microdomains, are affected by their absolute and relative abundances. Our data suggesting the functional interaction between the components of the 5-HT_{2A}–mGlu2 heteromer in the mouse and human frontal cortex provide an insight into the molecular basis by which these two receptors interact in native tissue. However, the use of different experimental approaches used in the different studies may provide an explanation for the absence of functional and pharmacological differences previously observed between cells expressing 5-HT_{2A} alone, mGlu2 alone, or 5-HT_{2A} and mGlu2 together (47).

In this context, one of the limitations of experiments performed in heterologous expression systems relates to the absolute and relative abundances of each receptor and whether findings from these in vitro experiments can be validated in native tissue and whole animal models. The experiments that we performed with HEK 293 cell lines were consistent with those performed with *Xenopus* oocytes (24). For example, LY379268 stimulated $G_{q/11}$-dependent signaling in cells expressing mGlu2 and 5-HT_{2A} receptors as a GPCR heteromer, and the relative ratio of GPCR protomers in the heteromeric complex was critical for the efficiency of its signaling crosstalk (24). However, there were also differences between the two experimental systems, such as the effects of PTX on the ability of mGlu2 to initiate crosstalk (24). Although the reasons underlying the differences in the two systems need to be further explored, the major conclusions from both sets of experimental conditions are consistent and applicable to native tissues. Similarly, although our previous work demonstrated that the activation of 5-HT_{2A} receptors by hallucinogens stimulates both $G_{q/11}$- and $G_{i/o}$-dependent signaling in cells expressing the 5-HT_{2A}–mGlu2 heteromer (22), detailed structural information about this crosstalk remains to be determined. We are also generating HEK 293 cell lines that stably coexpress mGlu2 and 5-HT_{2A} receptors at different relative abundances to define the basic mechanisms that govern the formation and function of receptor heteromers.

The frontal cortex is a region of the brain that is involved in critical processes, such as sensorimotor gating, cognition, and perception. Previous data suggested that the activation of mGlu2 autoreceptors mediates the presynaptic effects of mGlu2/3 receptor agonists in suppressing the electrophysiological effects of hallucinogenic 5-HT_{2A} receptor agonists recorded in postsynaptic cortical pyramidal neurons (49, 50). Our finding that 5-HT_{2A} and mGlu2 receptors are likely coexpressed as heteromers complex at the PSD in the cerebral cortex is not mutually exclusive with these findings. Our data, however, provide additional evidence that, together with previous observations that demonstrated coimmunoprecipitation in mouse (24) and human (22) frontal cortex and the physical proximity of 5-HT_{2A} and mGlu2 receptors at cortical synaptic junctions as determined by electron microscopy (23), support the existence of an alternative pathway through which these two receptor subtypes crosstalk in the central nervous system.

Although it is not without controversy (51, 52), preclinical and clinical studies suggest that the activation of mGlu2 by orthosteric mGlu2/3 agonists or allosteric mGlu2 agonists represents a new approach to treat schizophrenia and other psychotic disorders (39, 53–55). Through mouse models of psychosis, we showed that the expression of the 5-HT_{2A} receptor is at least in part necessary for the mGlu2-dependent antipsychotic-like behavioral effects of the mGlu2/3 receptor agonist LY379268 (24). Given that we showed that the activation of $G_{q/11}$ signaling by LY379268 was substantially reduced in the frontal cortex of 5-HT_{2A} knockout mice compared to that in wild-type mice, the selective reduction in the LY379268-dependent activation of $G_{q/11}$ coupling in frontal cortex of schizophrenic subjects suggests that alterations in signaling processes through the 5-HT_{2A}–mGlu2 heteromeric receptor complex may be involved in some of the psychotic symptoms in schizophrenia patients. In addition, considering that chronic treatment with atypical antipsychotic drugs epigenetically represses the promoter activity of the *mGlu2* (*Grm2*) gene in mouse and human frontal cortex through a molecular mechanism that requires 5-HT_{2A} receptor–dependent signaling (40), our current findings that suggest that the pattern of G protein coupling is affected by the organization of 5-HT_{2A} and mGlu2 receptors into heteromers may provide an explanation for why schizophrenia patients previously treated chronically with atypical antipsychotic drugs fail to respond to treatment with the mGlu2/3 receptor agonist pomaglumetad (LY2140023 prodrug of LY404039). This notion has been supported by clinical testing in schizophrenia patients (56).

In conclusion, we found that functional coupling of $G_{i/o}$ proteins to the mGlu2 protomer distal from the 5-HT_{2A} receptor is required for the mGlu2 component of the 5-HT_{2A}–mGlu2 heteromeric receptor complex to crosstalk with the 5-HT_{2A} receptor and consequently activate $G_{q/11}$-dependent signaling and Ca^{2+} release in live mammalian cells. These findings extend our understanding of the structural changes that underlie the pharmacology and function of GPCR heteromers and could be relevant for the development of new compounds to treat schizophrenia.

Materials and Methods

Drugs

5-Hydroxytryptamine hydrochloride (serotonin hydrochloride; 5-HT), GTPγS, and PTX were purchased from Sigma-Aldrich. (1*R*,4*R*,5*S*,6*R*)-4-Amino-2-oxabicyclo[3.1.0]hexane-4,6-dicarboxylic acid (LY379268), (2*S*)-2-amino-2-[(1*S*,2*S*)-2-carboxycycloprop-1-yl]-3-(xanth-9-yl) propanoic acid (LY341495), methysergide, L-glutamic acid, U73122, and NF023 were obtained from Tocris Bioscience. (1*R*,4*S*,5*S*,6*S*)-4-[[(2*S*)-2-Amino-4-(methylthio)-1-oxobutyl]amino]-2-thiabicyclo[3.1.0]hexane-4,6-dicarboxylic acid 2,2-dioxide (LY404039) was obtained from Selleckchem. The Gβγ-blocking peptide (MPS phosducin-like protein C-terminus: AAVALLPAVLLALLAVTDQLGEDFFAVDLEAFLQEFGLLPEKE) was obtained from AnaSpec. UBO-QIC (also known as FR900359) was purchased from the Institute of Pharmaceutical Biology, University of Bonn. M100,907 (volinanserin) was obtained from Sanofi. [^{3}H]Ketanserin and [^{35}S]GTPγS were obtained from PerkinElmer Life and

Analytical Sciences Inc. [H]LY341495 was purchased from American Radiolabeled Chemicals Inc. All other chemicals were obtained from standard sources.

Plasmid construction

All PCR assays were performed with PfuUltra Hotstart DNA Polymerase (Stratagene) in a Mastercycler Ep Gradient Auto thermal cycler (Eppendorf). Cycling conditions were 30 cycles of 94°C for 30 s, 55°C for 30 s, and 72°C for 1 min/kb of amplicon, with an initial denaturation/activation step of 94°C for 2 min and a final extension step of 72°C for 7 min. The following constructs have previously been described: pcDNA3.1–c-Myc–5-HT_{2A}–mCherry, pcDNA3.1-HA-mGlu2-eYFP, pcDNA3.1-HA-mGlu3-eYFP, pcDNA3.1-HA-mGlu2ΔTM4N-eYFP, and pcDNA3.1-HA-mGlu3ΔTM4,5-eYFP (22, 23). Introduction of the mutation I181D into the ICL2 of 5-HT_{2A}, the mutation F756S into the ICL3 of mGlu2, and the mutations Y216A and D295A into the binding pocket of mGlu2 were performed with the QuikChange II Site Directed Mutagenesis Kit according to the manufacturer's protocol (Stratagene). All of the constructs were confirmed by DNA sequencing. To generate the C-terminally c-Myc-tagged form of wild-type human 5-HT_{2C}, a PCR fragment was obtained using pcDNA3.1-5-HT_{2C} from the cDNA Resource Center (Missouri University of Science and Technology) as a template and the primers h5-HT_{2C}–Bmg BI/S (5′-AACACGACGTGCGTGCTCAACG-3′) and c-Myc-h5-HT_{2C}–Xba I/A (5′-TCTAGATCACAGATCTTCTTCAGAAATAAGTTTTTGTTCCACACTGCTAATCCTTTCGC-3′). The PCR product was digested with Bmg BI and Xba I and subcloned into the same restriction sites of pcDNA3.1–5-HT_{2C}. To generate the chimeric human 5-HT_{2A} with TM1 from human 5-HT_{2C}, we used PCR-directed mutagenesis. Two overlapping PCR fragments were obtained using pcDNA3.1–c-Myc–5-HT_{2A} as a template and the primers h5-HT_{2C}–TM1/S (5′-GGGGTACAAAACTGGCCAGCACTTTCAATCGTCATCATAATAATCATGACAATAGGTGGCAACATCCTTGTGATCATGGCAGTAAGCATGGAGAAAAAGCTGCAGAATGCCACC-3′) and h5-HT_{2C} –TM1/A (5′-CATGCTTACTGCCATGATCACAAGGATGTTGCCACCTATTGTCATGATTATTATGATGACGATTGAAAGTGCTGGCCAGTTTTGTACCCCGAGATGAAGTAAGGAGAGAC-3′). The final amplification product [1500 base pairs (bp)], which includes the mutant sequence in TM4 of human 5-HT_{2C}, was generated with the outer oligonucleotides Nhe I–h5-HT_{2A}/S (5′-TTTTGCTAGCATGGAACAAAAACTTATTTCTG-3′) and Bam HI–h5-HT_{2A}/A (5′-AAAAGGATCCTCACACACAGCTCACCTTTTC-3′). The final PCR product was digested with Nhe I and Bam HI and subcloned into the same restriction sites of pcDNA3.1–c-Myc–5-HT_{2A}. To generate chimeric human 5-HT_{2A} with TM4 from human 5-HT_{2C}, two overlapping PCR fragments were obtained using pcDNA3.1–c-Myc–5-HT_{2A} as a template and the primers h5-HT_{2C} –TM4/S (5′-CCATCATGAAGATTGCTATTGTTTGGGCAATTTCTATAGGTGTATCAGTTCCTATCCCTGTGTTTGGGCTACAGGACGATTCGAAGG-3′) and h5-HT_{2C}–TM4/A (5′-CACAGGGATAGGAACTGATACACCTATAGAAATTGCCCAAACAATAGCAATCTTCATGATGGCCTTAGTTCTGGAGTTGAAGC-3′). The final amplification product (1500 bp), which includes the mutant sequence in TM4 of human 5-HT_{2C}, was generated with the outer oligonucleotides Nhe I–h5-HT_{2A}/S (5′-TTTTGCTAGCATGGAACAAAAACTTATTTCTG-3′) and Bam HI-h5-HT_{2A}/A (5′-

AAAAGGATCCTCACACACAGCTCACCTTTTC-3′). The final PCR product was digested with Nhe I and Bam HI and subcloned into the same restriction sites of pcDNA3.1–c-Myc–5-HT2A. For 3-FRET experiments, the complementary DNAs (cDNAs) encoding Cerulean, mCitrine, and mCherry were amplified by PCR from their original vectors with the following primers: Not I–eYFP/S (5′-TTTTgcggccgcATGGTGAGCAAGGGCGAGGA-3′) and Xba I–eYFP/A (5′-TTTTtctagaTTACTTG-TACAGCTCGTCCA-3′). The PCR products were digested with Not I and Xba I and subcloned into the same sites of pcDNA3.1. The cDNAs encoding c-Myc–5-HT_{2A} C-terminally tagged with enhanced cyan fluorescent protein (eCFP) and HA-mGlu2 C-terminally tagged with eYFP (22) were digested with Nhe I and Bam HI and subcloned into the same restriction sites of pcDNA3.1-Cerulean, pcDNA3.1-mCitrine, or pcDNA3.1-mCherry. The mutant mCitrine-$Y^{67}C$ [a nonfluorescent variant of mCitrine (57)] was constructed with the QuikChange II Site Directed Mutagenesis Kit. For BiFC studies, constructs were generated by subcloning the sequence encoding the N-terminal 172–amino acid fragment or the C-terminal 67–amino acid fragment of mCitrine. Overlapping PCR fragments were obtained using pcDNA3.1-mCitrine as template and the primers Not I–eCFP/S (5′-TTTT gcggccgcATGGTGAGCAAGGGCGAGGA-3′) and Xba I–N–eCFP/A (5′-TTTTtctagaTTAGATGTTGTGGCGGATCT-3′) to subclone the N-terminal fragment of mCitrine, and the primers Not I–C–eCFP/S (5′-TTTTgcggccgcATGGAGGACGGCAGCGTGCA-3′) and Xba I–eCFP/A (5′-TTTTtctagaTTAGATGTTGTGGCGGATCT-3′) to subclone the C-terminal fragment of mCitrine. The PCR products were digested with Not I and Xba I and subcloned into the same sites of pcDNA3.1 to obtain the constructs pcDNA3.1–mCi-N172 and pcDNA3.1–mCi-C67. The form of HA-mGlu2 C-terminally tagged with eYFP (22) was digested with Nhe I and Bam HI and subcloned into the same restriction sites of pcDNA3.1–mCi-N172 and pcDNA3.1–mCi-C67 to generate pcDNA3.1–HA–mGlu2–mCi-N172 and pcDNA3.1–HA-mGlu2–mCi-C67.

Transient transfection of HEK 293 cells

HEK 293 cells were maintained in Dulbecco's modified Eagle's medium (DMEM; glucose, 4.5 g/liter) supplemented with 10% (v/v) dialyzed fetal bovine serum (FBS) at 37°C in a 5% CO_2 humidified atmosphere. Experiments were performed with dialyzed FBS to exclude the serotonin and glutamate that nondialyzed FBS may contain. Transfection was performed with the Lipofectamine 2000 reagent (Invitrogen) according to the manufacturer's instructions. The efficiency of cotransfection of eYFP- and mCherry-tagged constructs was 56.48 ± 9.89%.

Measurement of $[Ca^{2+}]_i$

HEK 293 cells were transfected with the appropriate combination of expression plasmids as indicated in the figure legends; pcDNA3.1 (empty vector) was used to normalize the amounts of plasmid DNA in each transfection. Twenty-four hours later, cells were harvested and plated onto Delta T culture dishes (catalog no. 04200415B; Bioptechs Inc.) where they were cultured for an additional 24 hours before experiments were performed. Transfected cells were loaded with the Ca^{2+}-sensitive dye Fura-2 (2.0 μM, catalog no. F1225; Life Technologies) and incubated for 45 min at 37°C under reduced light in Hanks' balanced salt solution (HBSS; catalog no. 14175; Life Technologies) and 0.04% Pluronic acid F-127

(catalog no. P6867; Invitrogen). Cells were incubated in HBSS for 20 min at 37°C under reduced light before experiments were performed. Cells were illuminated excited and imaged with an inverted epifluorescence microscope system (Olympus IX-70) equipped with a 20× objective (numerical aperture, 0.45) and a Uniblitz shutter, which was used to rapidly alternate the excitation wavelengths between 340 and 380 nm. Fura-2 fluorescence emission at 510 nm was monitored with an Evolution QEi CCD monochrome camera. MetaMorph imaging software was used to control all electronic hardware and image data processing. Sequential images were collected every 5 s, exposure to excitation was 200 ms per image, and all the experiments were performed in HBSS. Only individual cells that expressed detectable amounts of the respective fluorescent proteins (eYFP, mCherry, or both) were scored. Ratio images were presented in MetaMorph display mode, which associates the color hue with the excitation ratio value and the intensity of each hue with the source image brightness. Background fluorescence was subtracted from each raw image as follows. A region of interest was manually drawn in a region of no fluorescence adjacent to the fluorescent cells in the 380-nm channel image and then selected and transferred to the matched image acquired at 340 nm. The background amount was then subtracted from each pixel in each channel. Background-subtracted images were then used to calculate the 340/380 nm ratio of each pixel, which was used to indicate changes in $[Ca^{2+}]_i$. After determination of the upper and lower thresholds, the ratio value of each pixel was associated with 1 of the 24 hues from blue (low $[Ca^{2+}]_i$) to red (high $[Ca^{2+}]_i$). The pooled average intensity-modulated display ratio measured from single cells was expressed as the mean of at least 20 cells with the vertical lines representing SEM.

FCM-based FRET

FCM-based FRET assays were performed as previously described (23).

Coimmunoprecipitation assays

Coimmunoprecipitation assays were performed as previously described (23).

3-FRET in living cells

3-FRET assays were performed as previously reported with minor modifications (26). Briefly, to detect 3-FRET in living cells, six filter channel combinations were established (that is, mCherry: excitation = 580/10 nm, emission = 630/60 nm; mCitrine: excitation = 459/9 nm, emission = 535/30 nm; Cetrine: excitation = 425/10 nm, emission = 535/30; Cetrine/mCitrine/FRET: excitation = 425/10 nm, emission = 535/30 nm; Cetrine/mCitrine/mCherry/FRET: excitation = 424/10 nm, emission = 630/60 nm; and mCitrine/mCherry/FRET: excitation = 495/9 nm, emission = 630/60 nm), which enabled the acquisition of images from all three protein fluoro-phores and three raw FRET images. These images were used to calculate three corrected FRET images. MetaMorph imaging software was used to quantify the FRET images and to apply the necessary algorithms, pixel-by-pixel–based, to obtain a final image corresponding to the corrected and normalized FRET. Signal correction and normalization in 3-FRET was defined as previously reported (26).

Molecular modeling

Active conformations of homology models of the mGlu2 and 5-HT_{2A} receptors were built on the basis of the crystal structure of the β_2-adrenergic receptor–G_s protein complex (Protein Data Bank ID: 3SN6) (58). The CRUSTALW server was used for sequence alignments, and this was followed by manual adjustment. Three-dimensional (3D) molecular models were generated with the program Modeller V9.5 (59). Ten homology models for each mGlu2 and 5-HT_{2A} were generated, and model selection was performed on the basis of the internal DOPE (discrete optimized protein energy) scores in the Modeller program (60). 2D Brownian dynamics (2D BD) simulations were performed with the selected mGlu2 and 5-HT_{2A} models (61, 62). One million 2D BD simulations were conducted on each of the mGlu2-mGlu2, 5-HT_{2A}–5-HT_{2A}, and 5-HT_{2A}–mGlu2 homodimers and heterodimers. More than 120,000 complex models were obtained for each dimer from the 2D BD simulations. These results were filtered by adding restraints that enabled TM1, TM4, and TM1 domains to be located at the dimer interface for mGlu2-mGlu2, 5-HT_{2A}–mGlu2, and 5-HT_{2A}–5-HT_{2A}, respectively. The final dimer models were selected by visual inspection with the VMD (visual molecular dynamics) program (63). The mGlu2-mGlu2–5-HT_{2A}-5-HT_{2A} heteromer complexed with G_i and G_q was generated by superposition of the homodimers with the crystal structure of the β_2-adrenergic receptor–G_s protein complex using the Chimera program (64).

[^{3}H]Ketanserin, [^{3}H]LY341495, and [^{35}S]GTPγS binding assays in HEK 293 cells

Membrane preparations and [^{3}H]ketanserin and [^{3}H]LY341495 binding assays were performed as previously reported with minor modifications (22, 23). [^{35}S]GTPγS binding experiments were initiated by the addition of membranes containing 35 μg of protein to an assay buffer [1 mM EGTA, 3 mM $MgCl_2$, 100 mM NaCl, 0.2 mM dithiothreitol (DTT), 50 mM tris-HCl (pH 7.4), and 0.5 nM [^{35}S]GTPγS], supplemented with 50 μM GDP, and containing the concentrations of ligands indicated in the figure legends. Nonspecific binding was determined in the presence of 10 μM GTPγS. Membrane preparations were incubated at 30°C for 2 hours, and incubations were terminated by dilution with 3 ml of ice-cold incubation buffer. Free ligand was separated from bound ligand by rapid filtration under vacuum through GF/C glass fiber filters. The filters were then rinsed twice with 3 ml of ice-cold incubation buffer, air-dried, and counted for radioactivity by liquid scintillation spectrometry using a Betaplate counter (Wallac-PerkinElmer).

Whole-cell patch-clamp recordings in HEK 293 cells stably expressing GIRK

$G_{i/o}$-dependent signaling can be detected through GIRK channels (35). This is a subfamily of Kir (inwardly rectifying K^+) channels (or Kir3), which is sensitive to the Gβγ subunits of $G_{i/o}$ proteins. Experiments were performed in HEK 293 cells stably transfected with pBI-CMV1-GIRK1-GIRK4. Whole-cell patch-clamp current recordings were performed with a Patch Clamp L/M-EPC7 amplifier and Axon 8.1 software (Axon Instruments). Cells were trypsinized, resuspended in DMEM, and placed in the CO_2 incubator for at least 3 hours for recovery. After recovery, the cells were placed on poly-D-lysine coverslips, left to attach for ~15 min, and transferred to the chamber of the patch-clamp setup with a bath solution containing 140 mM potassium gluconate, 2 mM $CaCl_2$, 5 mM EGTA/KOH, 10 mM D-

glucose, 10 mM Hepes-K, and 1 mM $MgCl_2$. The composition of the pipette solution was 140 mM potassium gluconate, 2 mM $CaCl_2$, 5 mM EGTA/KOH, 10 mM D-glucose, 10 mM Hepes-K, 0.3 mM $MgCl_2$, 2 mM NaATP, 0.1 mM GTPγS, and, when appropriate, 0.01 mM MPS (the selective Gβγ blocker). Osmolarity in both solutions was 340 mosmol, and the pH was 7.4. Upon formation of the whole-cell configuration, a voltage ramp from −100 mV to +100 mV was applied, and data were collected. At the end of the recordings, 4 mM $BaCl_2$ was applied to block potassium currents. The first few data points of the current versus time plot at −100 mV were averaged to obtain the basal current. Similarly, GTPγS-induced currents were calculated by averaging several current values at the peak of the effect. Values were divided by the membrane capacitance (pF) to normalize for the size of each cell. The basal current was subtracted from the GTPγS-induced current, and the difference was divided by the basal current.

Experimental animals

Experiments were performed on adult (10- to 14-week-old) male mice. 5-HT_{2A} knockout (*Htr2a*$^{-/-}$) mice of 129S6/Sv background have been previously described (65). mGlu2 knockout (*Grm2*$^{-/-}$) mice were obtained from the RIKEN BioResource Center, Japan (66), and backcrossed for at least 10 generations onto the 129S6/Sv background (67). For experiments involving genetically modified mice, wild-type littermates were used as controls. The Institutional Animal Use and Care Committee at the Icahn School of Medicine at Mount Sinai approved all of the experimental procedures.

Subcellular fractionation and PSD isolation

Subcellular fractionation was performed as previously described, with minor modifications (68). Briefly, mice were sacrificed by cervical dislocation. Bilateral frontal cortex samples (bregma 1.90 to 1.40 mm) from two mice were homogenized in 1.5 ml of 0.32 M sucrose, 0.1 mM $CaCl_2$ containing protease and phosphatase inhibitors (Sigma-Aldrich). The homogenate was brought to a final concentration of 1.25 M sucrose by adding 2 M sucrose and 0.1 mM $CaCl_2$. The homogenate was then placed in an ultracentrifuge (Optima XE-100 Ultracentrifuge, Beckman Coulter), overlaid with 1 M sucrose, and subjected to centrifugation at 100,000*g* for 3 hours at 4°C. The synaptosomal fraction was collected at the interface between the 1.25 and 1 M sucrose solutions. To obtain the synaptic junctions, the synaptosomal fraction was diluted with 20 mM tris-HCl, 0.1 mM $CaCl_2$ (pH 6.0) containing 1% Triton X-100, mixed for 20 min at 4°C, and then centrifuged at 40,000*g* for 20 min at 4°C. The pellet containing the isolated synaptic junctions was collected. To separate presynaptic proteins from the PSD, the pellet was resuspended in 20 mM tris-HCl (pH 8.0), 0.1 mM $CaCl_2$, containing 1% Triton X-100. The mixture was again mixed for 20 min at 4°C and centrifuged at 40,000*g* for 20 min at 4°C. The insoluble pellet containing the PSD fraction and the supernatant containing the presynaptic fraction were collected at stored at −80°C until use.

Western blotting

For Western blotting analysis, equal amounts of proteins (150 μg) were resolved by 10% SDS-PAGE and transferred to nitrocellulose membranes by electroblotting. Detection of proteins by Western blotting with anti-mGlu2 (catalog no. ab15672; Abcam), anti–5-HT_{2A}

(catalog no. RA24288; Neuromics), anti–β-actin (catalog no. ab8227; Abcam), anti-PSD95 (catalog no. 2507; Cell Signaling), and anti–syntaxin-1 (catalog no. AB5820; Millipore) antibodies was performed with the enhanced chemiluminescence system according to the manufacturer's instructions. The specificity of the primary antibody (catalog no. ab15672; Abcam) against mGlu2 receptors was previously confirmed in experiments with knockout mice (23, 24). For confirmation of specificity of the primary antibody (catalog no. RA24288; Neuromics) against 5-HT_{2A} receptors in experiments with knockout mice, see fig. S9.

Immunocytochemistry

Experiments were performed as previously reported (23).

Postmortem human brain tissue samples

Human brains were obtained at autopsies performed between 1995 and 2007 in the Basque Institute of Legal Medicine, Bilbao, Spain, in compliance with policies of research and ethical boards for postmortem brain studies. Deaths were subjected to retrospective searching for previous medical diagnosis and treatment using examiner's information and records of hospitals and mental health centers. After searching of antemortem information was fulfilled, 27 subjects who had met the criteria of schizophrenia according to the Diagnostic and Statistical Manual of Mental Disorders (DSM-IV) were selected. A toxicological screening for antipsychotics, other drugs, and ethanol was performed on blood, urine, liver, and gastric content samples. Subjects who gave negative results for antipsychotic drugs in the toxicological screening were considered to be antipsychotic-free at death. The toxicological assays were performed at the National Institute of Toxicology, Madrid, Spain, with various standard procedures, including radioimmunoassay, enzymatic immunoassay, high-performance liquid chromatography, and gas chromatography–mass spectrometry. Controls for the present study were chosen among the collected brains on the basis, whenever possible, of the following cumulative criteria: (i) negative medical information on the presence of neuropsychiatric disorders or drug abuse; (ii) appropriate gender, age, postmortem delay (time between death and autopsy), and freezing storage time to match each subject in the schizophrenia group; (iii) sudden and unexpected death (motor vehicle accidents); and (iv) toxicological screening for psychotropic drugs with negative results except for ethanol. Specimens of prefrontal cortex (Brodmann's area 9) were dissected at autopsy (0.5 to 1 g of tissue) on an ice-cooled surface and immediately stored at −80°C until required for use. The definitive pairs of antipsychotic-free schizophrenics, antipsychotic-treated schizophrenics, and respective matched controls are shown in table S1. Pairs of samples from schizophrenia patients and matched controls were processed simultaneously and under the same experimental conditions. Brain samples were assayed for pH and RNA integrity number as previously reported (see table S1) (69).

Scintillation proximity assay for [^{35}S]GTPγS binding in mouse and human frontal cortex

Membrane preparations were performed as previously reported (70). [^{35}S]GTPγ S binding assays were performed in 96-well isoplates (Perkin-Elmer). [^{35}S]GTPγS binding experiments were initiated by the addition of membrane preparations containing 15 μg of protein to an assay buffer [1 mM EGTA, 3 mM $MgCl_2$, 100 mM NaCl, 1.0 mM DTT, 50

mM tris-HCl (pH 7.4), and 0.4 nM [^{35}S]GTPγS], supplemented with either 100 μM GDP (for anti-G$\alpha_{i1,2,3}$ experiments) or 50 μM GDP (anti-G$\alpha_{q/11}$ experiments), and containing the concentrations of ligands indicated in the figure legends (for a final volume of 200 μl per well). Nonspecific binding was determined in the presence of 100 μM GTPγS. Membrane preparations were incubated at 30°C for 2 hours with gentle agitation (450 rpm; ELMI Digital Thermostatic Shaker DTS-4), after which 20 μl of detergent solution (1.0% Igepal, 0.1% sodium deoxycholate, and protease inhibitors) was added and samples were then incubated at 22°C for 30 min with gentle agitation (400 rpm). After solubilization, 10 μl of either anti-G$\alpha_{i12,3}$ (sc-262) or anti-G$\alpha_{q/11}$ (sc-392) antibody was added at a 1:20 dilution and incubated at 22°C for 90 min. Finally, after the addition of 50 μl of scintillation proximity assay (SPA) polyvinyltoluene protein A SPA beads (2:3 dilution; PerkinElmer), the plates were incubated at 22°C for 2 hours with gentle agitation. Plates were centrifuged at 1000*g* for 15 min, and the scintillation signal was measured with a MicroBeta TriLux scintillation counter (PerkinElmer).

Statistical analysis

All statistical analyses were performed with GraphPad Prism software version 6. Concentration-response curves (Figs. 1, E and I, 2L, and 3D) were analyzed with the following equation: $Y = Y_{min} + (Y_{max} - Y_{min}) \cdot [X]/([X] + K_{0.5})$. Restricting the parameter Y_{min} to be zero, the equation was also used to fit the nonlinear curve for the radioligand binding saturation curves (fig. S7), with Y_{max} renamed as Bmax, and for the FCM-based FRET data (fig. S6, A and C), with Ymax renamed as $FRET_{max}$. An extra sum of square (*F* test) was used to determine the statistical difference for the simultaneous analysis of binding saturation curves (fig. S7), FCM-based FRET data (fig. S6, A and C), and concentration-response curves (Figs. 1, E and I, 2L, and 3D). The statistical significance of experiments involving two groups was assessed by Student's *t* test, whereas the statistical significance of experiments involving three or more groups was assessed by one-way ANOVA followed by Bonferroni's post hoc test. The statistical significance of experiments involving three or more groups and two or more experimental conditions was assessed by two-way ANOVA followed by Bonferroni's post hoc test. The level of significance was chosen at $P = 0.05$. All data are presented as means ± SEM.

Supplementary Material

Refer to Web version on PubMed Central for supplementary material.

Acknowledgments

We thank M. Fribourg for critical review of the manuscript, J. M. Eltit for insightful discussions, H. Vaananen for assistance with GIRK current graph preparation, R. Huq for help in Ca^{2+} signaling assays at the Microscopy Core, J. Gingrich for the gift of 5-HT_{2A} knockout mice, and the staff members of the Basque Institute of Legal Medicine for their cooperation in the study.

Funding: This work was supported, in whole or in part, by the NIH grants R01MH084894 and R56MH084894 (to J.G.-M.), R01HL59949 (to D.E.L.), R37AG017926 and R01AG008200 (to N.K.R.), R01DA025036 and R01DA027460 (to J.A.M.), R01NS047229 and P50AG05138 (to A.G.), and S10RR027411 (to M.C.). This work was also supported by Dainippon Sumitomo Pharma (to J.G.-M.), Spanish MINECO/EDR Funds SAF2009-68460 and SAF2013-48586R (to J.J.M.), the Basque Government (to J.J.M.), the Spanish Government SAF2010-15663 grant (MICINN) (to J.F.L.G.), and Medical Research Council (UK) grants MR/L023806/1 and G0900050 (to

G.M.). P.M.-A. and A.G.-B. were recipients of predoctoral fellowships from UPV/EHU and the Basque Government in Spain, respectively.

References and Notes

1. Rosenbaum DM, Rasmussen SGF, Kobilka BK. The structure and function of G-protein-coupled receptors. Nature. 2009; 459:356–363. [PubMed: 19458711]
2. Audet M, Bouvier M. Restructuring G-protein- coupled receptor activation. Cell. 2012; 151:14–23. [PubMed: 23021212]
3. Oldham WM, Hamm HE. Heterotrimeric G protein activation by G-protein-coupled receptors. Nat Rev Mol Cell Biol. 2008; 9:60–71. [PubMed: 18043707]
4. Whorton MR, Bokoch MP, Rasmussen SGF, Huang B, Zare RN, Kobilka B, Sunahara RK. A monomeric G protein-coupled receptor isolated in a high-density lipoprotein particle efficiently activates its G protein. Proc Natl Acad Sci USA. 2007; 104:7682–7687. [PubMed: 17452637]
5. Whorton MR, Jastrzebska B, Park PSH, Fotiadis D, Engel A, Palczewski K, Sunahara RK. Efficient coupling of transducin to monomeric rhodopsin in a phospholipid bilayer. J Biol Chem. 2008; 283:4387–4394. [PubMed: 18033822]
6. Kuszak AJ, Pitchiaya S, Anand JP, Mosberg HI, Walter NG, Sunahara RK. Purification and functional reconstitution of monomeric μ-opioid receptors: Allosteric modulation of agonist binding by G_{i2}. J Biol Chem. 2009; 284:26732–26741. [PubMed: 19542234]
7. Maurel D, Comps-Agrar L, Brock C, Rives ML, Bourrier E, Ayoub MA, Bazin H, Tinel N, Durroux T, Prézeau L, Trinquet E, Pin JP. Cell-surface protein-protein interaction analysis with time-resolved FRET and snap-tag technologies: Application to GPCR oligomerization. Nat Methods. 2008; 5:561–567. [PubMed: 18488035]
8. González-Maeso J. GPCR oligomers in pharmacology and signaling. Mol Brain. 2011; 4:20. [PubMed: 21619615]
9. Huang J, Chen S, Zhang JJ, Huang XY. Crystal structure of oligomeric β_1-adrenergic G protein–coupled receptors in ligand-free basal state. Nat Struct Mol Biol. 2013; 20:419–425. [PubMed: 23435379]
10. Manglik A, Kruse AC, Kobilka TS, Thian FS, Mathiesen JM, Sunahara RK, Pardo L, Weis WI, Kobilka BK, Granier S. Crystal structure of the μ-opioid receptor bound to a morphinan antagonist. Nature. 2012; 485:321–326. [PubMed: 22437502]
11. Wu B, Chien EYT, Mol CD, Fenalti G, Liu W, Katritch V, Abagyan R, Brooun A, Wells P, Bi FC, Hamel DJ, Kuhn P, Handel TM, Cherezov V, Stevens RC. Structures of the CXCR4 chemokine GPCR with small-molecule and cyclic peptide antagonists. Science. 2010; 330:1066–1071. [PubMed: 20929726]
12. Wu H, Wacker D, Mileni M, Katritch V, Han GW, Vardy E, Liu W, Thompson AA, Huang XP, Carroll FI, Mascarella SW, Westkaemper RB, Mosier PD, Roth BL, Cherezov V, Stevens RC. Structure of the human κ-opioid receptor in complex with JDTic. Nature. 2012; 485:327–332. [PubMed: 22437504]
13. Huang W, Manglik A, Venkatakrishnan AJ, Laeremans T, Feinberg EN, Sanborn AL, Kato HE, Livingston KE, Thorsen TS, Kling RC, Granier S, Gmeiner P, Husbands SM, Traynor JR, Weis WI, Steyaert J, Dror RO, Kobilka BK. Structural insights into μ-opioid receptor activation. Nature. 2015; 524:315–321. [PubMed: 26245379]
14. Carrillo JJ, Pediani J, Milligan G. Dimers of class A G protein-coupled receptors function via agonist-mediated trans-activation of associated G proteins. J Biol Chem. 2003; 278:42578–42587. [PubMed: 12920117]
15. Margeta-Mitrovic M, Jan YN, Jan LY. Ligand-induced signal transduction within heterodimeric $GABA_B$ receptor. Proc Natl Acad Sci USA. 2001; 98:14643–14648. [PubMed: 11724957]
16. Margeta-Mitrovic M, Jan YN, Jan LY. Function of GB1 and GB2 subunits in G protein coupling of $GABA_B$ receptors. Proc Natl Acad Sci USA. 2001; 98:14649–14654. [PubMed: 11724956]
17. Han Y, Moreira IS, Urizar E, Weinstein H, Javitch JA. Allosteric communication between protomers of dopamine class A GPCR dimers modulates activation. Nat Chem Biol. 2009; 5:688–695. [PubMed: 19648932]

18. Mesnier D, Baneres JL. Cooperative conformational changes in a G-protein-coupled receptor dimer, the leukotriene B_4 receptor BLT1. J Biol Chem. 2004; 279:49664–49670. [PubMed: 15358776]
19. Damian M, Mary S, Martin A, Pin JP, Banères JL. G protein activation by the leukotriene B_4 receptor dimer. Evidence for an absence of trans-activation. J Biol Chem. 2008; 283:21084–21092. [PubMed: 18490452]
20. Moreno JL, González-Maeso J. Preclinical models of antipsychotic drug action. Int J Neuropsychopharmacol. 2013; 16:2131–2144. [PubMed: 23745738]
21. Hanks JB, González-Maeso J. Animal models of serotonergic psychedelics. ACS Chem Neurosci. 2013; 4:33–42. [PubMed: 23336043]
22. González-Maeso J, Ang RL, Yuen T, Chan P, Weisstaub NV, López-Giménez JF, Zhou M, Okawa Y, Callado LF, Milligan G, Gingrich JA, Filizola M, Meana JJ, Sealfon SC. Identification of a serotonin/glutamate receptor complex implicated in psychosis. Nature. 2008; 452:93–97. [PubMed: 18297054]
23. Moreno JL, Muguruza C, Umali A, Mortillo S, Holloway T, Pilar-Cuéllar F, Mocci G, Seto J, Callado LF, Neve RL, Milligan G, Sealfon SC, López-Giménez JF, Meana JJ, Benson DL, González-Maeso J. Identification of three residues essential for 5-hydroxytryptamine 2A-metabotropic glutamate 2 ($5\text{-}HT_{2A}$·mGlu2) receptor heteromerization and its psychoactive behavioral function. J Biol Chem. 2012; 287:44301–44319. [PubMed: 23129762]
24. Fribourg M, Moreno JL, Holloway T, Provasi D, Baki L, Mahajan R, Park G, Adney SK, Hatcher C, Eltit JM, Ruta JD, Albizu L, Li Z, Umali A, Shim J, Fabiato A, MacKerell AD Jr, Brezina V, Sealfon SC, Filizola M, González-Maeso J, Logothetis DE. Decoding the signaling of a GPCR heteromeric complex reveals a unifying mechanism of action of antipsychotic drugs. Cell. 2011; 147:1011–1023. [PubMed: 22118459]
25. Takahashi A, Camacho P, Lechleiter JD, Herman B. Measurement of intracellular calcium. Physiol Rev. 1999; 79:1089–1125. [PubMed: 10508230]
26. Lopez-Gimenez JF, Canals M, Pediani JD, Milligan G. The α_{1b}-adrenoceptor exists as a higher-order oligomer: Effective oligomerization is required for receptor maturation, surface delivery, and function. Mol Pharmacol. 2007; 71:1015–1029. [PubMed: 17220353]
27. Urban JD, Clarke WP, von Zastrow M, Nichols DE, Kobilka B, Weinstein H, Javitch JA, Roth BL, Christopoulos A, Sexton PM, Miller KJ, Spedding M, Mailman RB. Functional selectivity and classical concepts of quantitative pharmacology. J Pharmacol Exp Ther. 2007; 320:1–13. [PubMed: 16803859]
28. González-Maeso J, Weisstaub NV, Zhou M, Chan P, Ivic L, Ang R, Lira A, Bradley-Moore M, Ge Y, Zhou Q, Sealfon SC, Gingrich JA. Hallucinogens recruit specific cortical $5\text{-}HT_{2A}$ receptor-mediated signaling pathways to affect behavior. Neuron. 2007; 53:439–452. [PubMed: 17270739]
29. Biber K, Klotz KN, Berger M, Gebicke-Härter PJ, van Calker D. Adenosine A_1 receptor-mediated activation of phospholipase C in cultured astrocytes depends on the level of receptor expression. J Neurosci. 1997; 17:4956–4964. [PubMed: 9185533]
30. Murthy KS, Zhou H, Huang J, Pentyala SN. Activation of PLC-δ1 by $G_{i/o}$-coupled receptor agonists. Am J Physiol Cell Physiol. 2004; 287:C1679–C1687. [PubMed: 15525688]
31. Schrage R, Schmitz AL, Gaffal E, Annala S, Kehraus S, Wenzel D, Büllesbach KM, Bald T, Inoue A, Shinjo Y, Galandrin S, Shridhar N, Hesse M, Grundmann M, Merten N, Charpentier TH, Martz M, Butcher AJ, Slodczyk T, Armando S, Effern M, Namkung Y, Jenkins L, Horn V, Stößel A, Dargatz H, Tietze D, Imhof D, Galés C, Drewke C, Müller CE, Hölzel M, Milligan G, Tobin AB, Gomeza J, Dohlman HG, Sondek J, Harden TK, Bouvier M, Laporte SA, Aoki J, Fleischmann BK, Mohr K, König GM, Tüting T, Kostenis E. The experimental power of FR900359 to study Gq-regulated biological processes. Nat Commun. 2015; 6:10156. [PubMed: 26658454]
32. Francesconi A, Duvoisin RM. Role of the second and third intracellular loops of metabotropic glutamate receptors in mediating dual signal transduction activation. J Biol Chem. 1998; 273:5615–5624. [PubMed: 9488690]
33. Freissmuth M, Boehm S, Beindl W, Nickel P, Ijzerman AP, Hohenegger M, Nanoff C. Suramin analogues as subtype-selective G protein inhibitors. Mol Pharmacol. 1996; 49:602–611. [PubMed: 8609887]

34. Orr AW, Pallero MA, Murphy-Ullrich JE. Thrombospondin stimulates focal adhesion disassembly through G_i- and phosphoinositide 3-kinase-dependent ERK activation. J Biol Chem. 2002; 277:20453–20460. [PubMed: 11923291]
35. Logothetis DE, Kurachi Y, Galper J, Neer EJ, Clapham DE. The βγ subunits of GTP-binding proteins activate the muscarinic K^+ channel in heart. Nature. 1987; 325:321–326. [PubMed: 2433589]
36. Kerppola TK. Visualization of molecular interactions by fluorescence complementation. Nat Rev Mol Cell Biol. 2006; 7:449–456. [PubMed: 16625152]
37. Kniazeff J, Bessis AS, Maurel D, Ansanay H, Prézeau L, Pin JP. Closed state of both binding domains of homodimeric mGlu receptors is required for full activity. Nat Struct Mol Biol. 2004; 11:706–713. [PubMed: 15235591]
38. El Moustaine D, Granier S, Doumazane E, Scholler P, Rahmeh R, Bron P, Mouillac B, Baneres JL, Rondard P, Pin JP. Distinct roles of metabotropic glutamate receptor dimerization in agonist activation and G-protein coupling. Proc Natl Acad Sci USA. 2012; 109:16342–16347. [PubMed: 22988116]
39. Moreno JL, Sealfon SC, González-Maeso J. Group II metabotropic glutamate receptors and schizophrenia. Cell Mol Life Sci. 2009; 66:3777–3785. [PubMed: 19707855]
40. Kurita M, Holloway T, Garcia-Bea A, Kozlenkov A, Friedman AK, Moreno JL, Heshmati M, Golden SA, Kennedy PJ, Takahashi N, Dietz DM, Mocci G, Gabilondo AM, Hanks J, Umali A, Callado LF, Gallitano AL, Neve RL, Shen L, Buxbaum JD, Han MH, Nestler EJ, Meana JJ, Russo SJ, González-Maeso J. HDAC2 regulates atypical antipsychotic responses through the modulation of *mGlu2* promoter activity. Nat Neurosci. 2012; 15:1245–1254. [PubMed: 22864611]
41. Muguruza C, Moreno JL, Umali A, Callado LF, Meana JJ, González-Maeso J. Dysregulated 5-HT_{2A} receptor binding in postmortem frontal cortex of schizophrenic subjects. Eur Neuropsychopharmacol. 2013; 23:852–864. [PubMed: 23176747]
42. Hlavackova V, Zabel U, Frankova D, Bätz J, Hoffmann C, Prezeau L, Pin JP, Blahos J, Lohse MJ. Sequential inter- and intrasubunit rearrangements during activation of dimeric metabotropic glutamate receptor 1. Sci Signal. 2012; 5:ra59. [PubMed: 22894836]
43. Bayburt TH, Leitz AJ, Xie G, Oprian DD, Sligar SG. Transducin activation by nanoscale lipid bilayers containing one and two rhodopsins. J Biol Chem. 2007; 282:14875–14881. [PubMed: 17395586]
44. Wu H, Wang C, Gregory KJ, Han GW, Cho HP, Xia Y, Niswender CM, Katritch V, Meiler J, Cherezov V, Conn PJ, Stevens RC. Structure of a class C GPCR metabotropic glutamate receptor 1 bound to an allosteric modulator. Science. 2014; 344:58–64. [PubMed: 24603153]
45. Xue L, Rovira X, Scholler P, Zhao H, Liu J, Pin JP, Rondard P. Major ligand-induced rearrangement of the heptahelical domain interface in a GPCR dimer. Nat Chem Biol. 2015; 11:134–140. [PubMed: 25503927]
46. Rives ML, Vol C, Fukazawa Y, Tinel N, Trinquet E, Ayoub MA, Shigemoto R, Pin JP, Prézeau L. Crosstalk between $GABA_B$ and mGlu1a receptors reveals new insight into GPCR signal integration. EMBO J. 2009; 28:2195–2208. [PubMed: 19590495]
47. Delille HK, Becker JM, Burkhardt S, Bleher B, Terstappen GC, Schmidt M, Meyer AH, Unger L, Marek GJ, Mezler M. Heterocomplex formation of 5-HT_{2A}-$mGlu_2$ and its relevance for cellular signaling cascades. Neuropharmacology. 2012; 62:2184–2191. [PubMed: 22300836]
48. Nygaard R, Zou Y, Dror RO, Mildorf TJ, Arlow DH, Manglik A, Pan AC, Liu CW, Fung JJ, Bokoch MP, Thian FS, Kobilka TS, Shaw DE, Mueller L, Prosser RS, Kobilka BK. The dynamic process of β_2-adrenergic receptor activation. Cell. 2013; 152:532–542. [PubMed: 23374348]
49. Marek GJ, Wright RA, Schoepp DD, Monn JA, Aghajanian GK. Physiological antagonism between 5-hydroxytryptamine$_{2A}$ and group II metabotropic glutamate receptors in prefrontal cortex. J Pharmacol Exp Ther. 2000; 292:76–87. [PubMed: 10604933]
50. Marek GJ, Wright RA, Gewirtz JC, Schoepp DD. A major role for thalamocortical afferents in serotonergic hallucinogen receptor function in the rat neocortex. Neuroscience. 2001; 105:379–392. [PubMed: 11672605]
51. Kinon BJ, Zhang L, Millen BA, Osuntokun OO, Williams JE, Kollack-Walker S, Jackson K, Kryzhanovskaya L, Jarkova N. HBBI Study Group. A multicenter, inpatient, phase 2, double-

blind, placebo-controlled dose-ranging study of LY2140023 monohydrate in patients with DSM-IV schizophrenia. J Clin Psychopharmacol. 2011; 31:349–355. [PubMed: 21508856]

52. Adams DH, Kinon BJ, Baygani S, Millen BA, Velona I, Kollack-Walker S, Walling DP. A long-term, phase 2, multicenter, randomized, open-label, comparative safety study of pomaglumetad methionil (LY2140023 monohydrate) versus atypical antipsychotic standard of care in patients with schizophrenia. BMC Psychiatry. 2013; 13:143. [PubMed: 23694720]
53. Patil ST, Zhang L, Martenyi F, Lowe SL, Jackson KA, Andreev BV, Avedisova AS, Bardenstein LM, Gurovich IY, Morozova MA, Mosolov SN, Neznanov NG, Reznik AM, Smulevich AB, Tochilov VA, Johnson BG, Monn JA, Schoepp DD. Activation of mGlu2/3 receptors as a new approach to treat schizophrenia: A randomized phase 2 clinical trial. Nat Med. 2007; 13:1102–1107. [PubMed: 17767166]
54. Kinon BJ, Gómez JC. Clinical development of pomaglumetad methionil: A non-dopaminergic treatment for schizophrenia. Neuropharmacology. 2013; 66:82–86. [PubMed: 22722029]
55. Ellaithy A, Younkin J, González-Maeso J, Logothetis DE. Positive allosteric modulators of metabotropic glutamate 2 receptors in schizophrenia treatment. Trends Neurosci. 2015; 38:506–516. [PubMed: 26148747]
56. Kinon BJ, Millen BA, Zhang L, McKinzie DL. Exploratory analysis for a targeted patient population responsive to the metabotropic glutamate 2/3 receptor agonist pomaglumetad methionil in schizophrenia. Biol Psychiatry. 2015; 78:754–762. [PubMed: 25890643]
57. Koushik SV, Chen H, Thaler C, Puhl HL III, Vogel SS. Cerulean, Venus, and VenusY67C FRET reference standards. Biophys J. 2006; 91:L99–L101. [PubMed: 17040988]
58. Rasmussen SGF, DeVree BT, Zou Y, Kruse AC, Chung KY, Kobilka TS, Thian FS, Chae PS, Pardon E, Calinski D, Mathiesen JM, Shah STA, Lyons JA, Caffrey M, Gellman SH, Steyaert J, Skiniotis G, Weis WI, Sunahara RK, Kobilka BK. Crystal structure of the β_2 adrenergic receptor–Gs protein complex. Nature. 2011; 477:549–555. [PubMed: 21772288]
59. Eswar N, Webb B, Marti-Renom MA, Madhusudhan MS, Eramian D, Shen MY, Pieper U, Sali A. Comparative protein structure modeling using Modeller. Curr Protoc Bioinformatics. 2006; Chapter 5 Unit 5.6.
60. Šali A, Blundell TL. Comparative protein modelling by satisfaction of spatial restraints. J Mol Biol. 1993; 234:779–815. [PubMed: 8254673]
61. Cui M, Mezei M, Osman R. Modeling dimerizations of transmembrane proteins using Brownian dynamics simulations. J Comput Aided Mol Des. 2008; 22:553–561. [PubMed: 18338226]
62. Meng XY, Mezei M, Cui M. Computational approaches for modeling GPCR dimerization. Curr Pharm Biotechnol. 2014; 15:996–1006. [PubMed: 25307013]
63. Humphrey W, Dalke A, Schulten K. VMD: Visual molecular dynamics. J Mol Graph. 1996; 14:27–38.
64. Pettersen EF, Goddard TD, Huang CC, Couch GS, Greenblatt DM, Meng EC, Ferrin TE. UCSF Chimera—A visualization system for exploratory research and analysis. J Comput Chem. 2004; 25:1605–1612. [PubMed: 15264254]
65. González-Maeso J, Yuen T, Ebersole BJ, Wurmbach E, Lira A, Zhou M, Weisstaub N, Hen R, Gingrich JA, Sealfon SC. Transcriptome fingerprints distinguish hallucinogenic and nonhallucinogenic 5-hydroxytryptamine 2A receptor agonist effects in mouse somatosensory cortex. J Neurosci. 2003; 23:8836–8843. [PubMed: 14523084]
66. Yokoi M, Kobayashi K, Manabe T, Takahashi T, Sakaguchi I, Katsuura G, Shigemoto R, Ohishi H, Nomura S, Nakamura K, Nakao K, Katsuki M, Nakanishi S. Impairment of hippocampal mossy fiber LTD in mice lacking mGluR2. Science. 1996; 273:645–647. [PubMed: 8662555]
67. Moreno JL, Holloway T, Albizu L, Sealfon SC, González-Maeso J. Metabotropic glutamate mGlu2 receptor is necessary for the pharmacological and behavioral effects induced by hallucinogenic 5-HT2A receptor agonists. Neurosci Lett. 2011; 493:76–79. [PubMed: 21276828]
68. Billa SK, Sinha N, Rudrabhatla SR, Morón JA. Extinction of morphine-dependent conditioned behavior is associated with increased phosphorylation of the GluR1 subunit of AMPA receptors at hippocampal synapses. Eur J Neurosci. 2009; 29:55–64. [PubMed: 19077125]
69. Garcia-Sevilla JA, Álvaro-Bartolomé M, Díez-Alarcia R, Ramos-Miguel A, Puigdemont D, Pérez V, Alvarez E, Meana JJ. Reduced platelet G protein-coupled receptor kinase 2 in major depressive

disorder: Antidepressant treatment-induced upregulation of GRK2 protein discriminates between responder and non-responder patients. Eur Neuropsychopharmacol. 2010; 20:721–730. [PubMed: 20493668]

70. González-Maeso J, Rodríguez-Puertas R, Meana JJ, García-Sevilla JA, Guimón J. Neurotransmitter receptor-mediated activation of G-proteins in brains of suicide victims with mood disorders: Selective supersensitivity of α_{2A}-adrenoceptors. Mol Psychiatry. 2002; 7:755–767. [PubMed: 12192620]

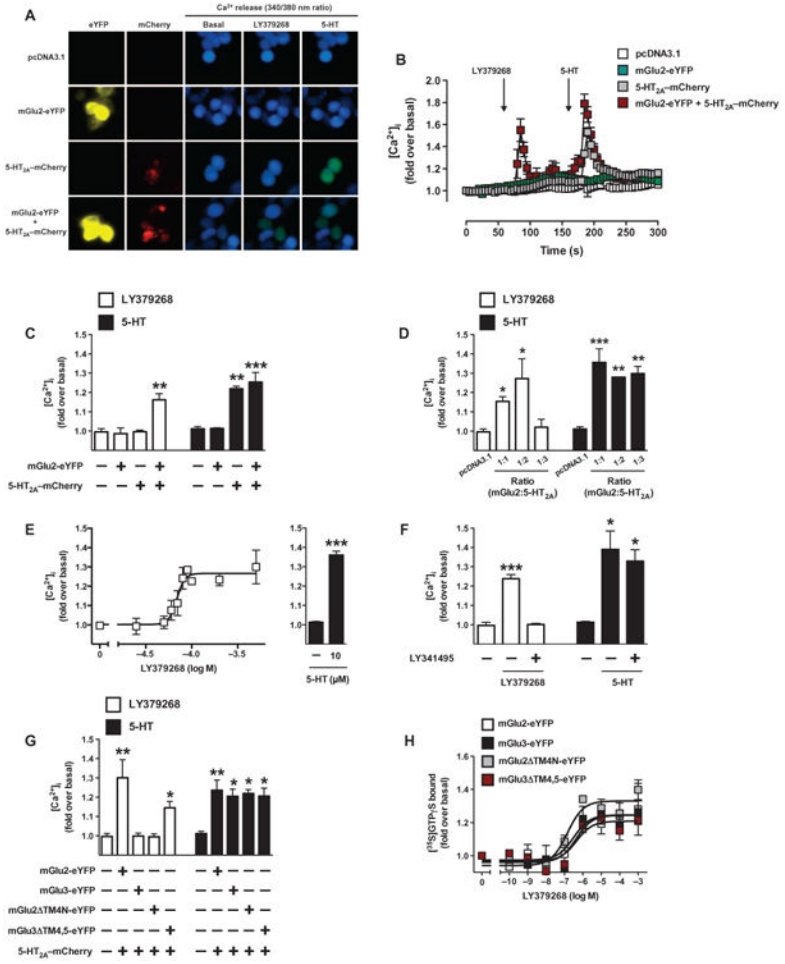

Fig. 1. The ability of the mGlu2/3 receptor agonist LY379268 to stimulate Ca^{2+} release requires the assembly of 5-HT_{2A}–mGlu2 hetero-mers in HEK 293 cells

(**A** to **C**) HEK 293 cells transfected with the control plasmid pcDNA3.1 or trans-fected with plasmids encoding mGlu2-eYFP and 5-HT_{2A}–mCherry alone or in combination were loaded with Fura-2 and monitored for $[Ca^{2+}]_i$ signals after sequential stimulation with 100 μM LY379268 (an mGlu2/3 receptor agonist) and 10 μM 5-HT. (A) Images captured before and after drug additions are representative of three independent experiments. (B) Time course of Ca^{2+} release in HEK 293 cells expressing the indicated constructs. The arrowheads indicate the times when the drugs were added. (C) Analysis of the fold increase in $[Ca^{2+}]_i$ in cells expressing the indicated combination of receptors. Data in (B) and (C) are means ± SEM of five to eight experiments. (**D**) HEK 293 cells transfected withpcDNA3.1 as a control or cotransfected with the indicated ratios of plasmids encoding eYFP - and mCherry-tagged receptors were sequentially stimulated withLY379268 and 5-HT before Ca^{2+} release was measured. Data aremeans ± SEM of three experiments. (**E**) HEK 293 cells cotransfected with plasmids encoding mGlu2-eYFP and 5-HT_{2A}–mCherry were stimulated with the indicated concentrations of LY379268 (left panel)and then with 5-HT (right panel)before Ca^{2+} release was measured. Data are means ± SEM of 3 to 10 experiments. (**F**) HEK 293 cells coexpressing mGlu2-eYFP and 5-HT_{2A}–mCherry were treated with vehicle (–) or were sequentially stimulated with LY379268 and 5-HT in the absence or presence of 10 μM

LY341495 (an mGlu2/3 receptor antagonist). Data are means ± SEM of three to five experiments. (**G**) HEK 293 cells transfected with control plasmid or cotransfected with plasmids encoding the indicated eYFP- and mCherry-tagged constructs were sequentially stimulated with LY379268 (white bars) and 5-HT (black bars) before Ca^{2+} release was measured. Data are means ± SEM of three to six experiments. $*P < 0.05$, $**P < 0.01$, and $***P < 0.001$ by Bonferroni's post hoc test of one-way analysis of variance (ANOVA) (C, D, G, and H) or by Student's *t* test (F). (**H**) LY379268-stimulated [^{35}S]GTPγS binding in plasma membrane preparations of HEK 293 cells transfected with plasmids encoding the indicated eYFP- or mCherry-tagged receptors. Data are means ± SEM of two or three experiments.

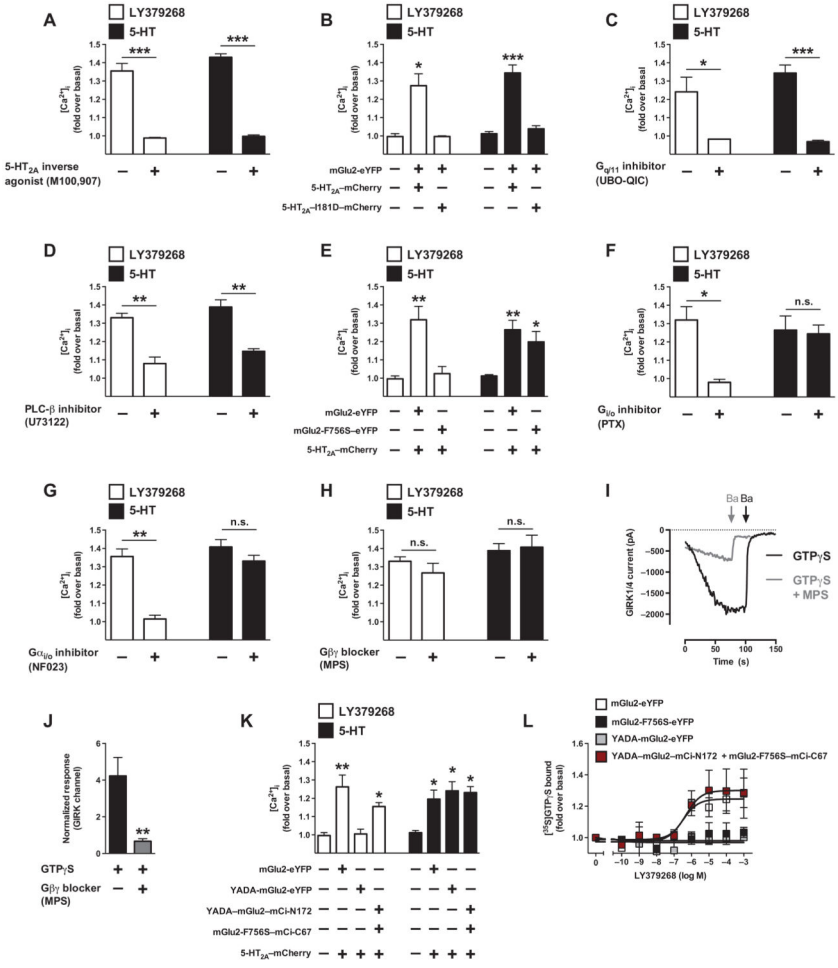

Fig. 2. Coupling to both $G_{i/o}$ and $G_{q/11}$ proteins is necessary for LY379268-induced Ca^{2+} release in HEK 293 cells expressing 5-HT_{2A}–mGlu2 heteromers

(**A**) Effect of 20-min pretreatment with 10 μM M100,907 on Ca^{2+} release in HEK 293 cells coexpressing mGlu2-eYFP and 5-HT_{2A}–mCherry after sequential stimulation with 100 μM LY379268 (white bars) and 10 μM 5-HT (black bars). (**B**) Measurement of Ca^{2+} release in HEK 293 cells transfected with control plasmid or coexpressing mGlu2-eYFP and either 5-HT_{2A}–mCherry or 5-HT_{2A}–I181D–mCherry after sequential stimulation with LY379268 and 5-HT. (**C**) Effect of 20-min pretreatment with 1 μM UBO-QIC (a selective $G_{q/11}$ inhibitor) or vehicle on Ca^{2+} release in HEK 293 cells coex-pressing mGlu2-eYFP and 5-HT_{2A}–mCherry after sequential stimulation with LY379268 and 5-HT. (**D**) Effect of 20-min pretreatment with 10 μM U73122 (a selective PLC-γ inhibitor) or vehicle on Ca^{2+} release in HEK 293 cells coexpressing mGlu2-eYFP and 5-HT_{2A}–mCherry after sequential stimulation with LY379268 and 5-HT. (**E**) Measurement of Ca^{2+} release in HEK293 cells transfected with control plasmid or coexpressing 5-HT_{2A}–mCherry with either mGlu2-eYFP or mGlu2-F756S–eYFP after sequential stimulation with LY379268 and 5-HT. (**F**) Effect of overnight incubation with PTX (500 ng/ml) or vehicle on Ca^{2+} release in HEK 293 cells coexpressing mGlu2-eYFP and 5-HT_{2A}–mCherry after sequential stimulation with LY379268 and 5-HT. (**G**) Effect of 30-min pretreatment with 10 μM NF023 (a selective $G\alpha_{i/o}$ inhibitor) or vehicle on Ca^{2+} release in HEK 293 cells coexpressing mGlu2-eYFP and

5-HT_{2A}–mCherry after sequential stimulation with LY379268 and 5-HT. (**H**) Effect of 60-min pretreatment with 10 μM MPS (a selective Gβγ blocker) or vehicle on Ca^{2+} release in cells coexpressing mGlu2-eYFP and 5-HT_{2A}–mCherry after sequential stimulation with LY379268 and 5-HT. (**I** and **J**) Effect of 10 μM MPS on G protein–coupled inwardly rectifying potassium (GIRK) currents in response to 100 μM GTPγS included in the patch pipette. Representative traces (I) and the summary of data (J) from whole-cell patch-clamp recordings show the membrane-permeable sequence (MPS)–dependent inhibition of GTPγS-induced GIRK currents in HEK 293 cells expressing GIRK1 and GIRK4. Barium (Ba) inhibited GIRK currents and enabled the subtraction of GIRK-independent currents. (**K**) Measurement of Ca^{2+} release in response to sequential stimulation with LY379268 and 5-HT in HEK 293 cells transfected with control plasmid or cotransfected with plasmids encoding the indicated eYFP- and mCherry-tagged constructs or with plasmids encoding the indicated mGlu2 mutant. Data are means ± SEM of 3 or 4 experiments (A, C, D, G, and H), 3 to 5 experiments (E), 4 or 5 experiments (F), 3 to 6 experiments (B and K), or 10 experiments (J). $*P < 0.05$, $**P < 0.01$, and $***P < 0.001$ by Bonferroni's post hoc test of one-way ANOVA (A to H and K) or Student's *t* test (J). (**L**) LY379268-stimulated [^{35}S]GTPγS binding in plasma membrane preparations of HEK 293 cells expressing the indicated eYFP- or mCherry-tagged receptors or coexpressing the indicated mCi-N172–or mCi-C67–tagged constructs. Data are means ± SEM of two or three experiments each performed in triplicate. n.s., not significant.

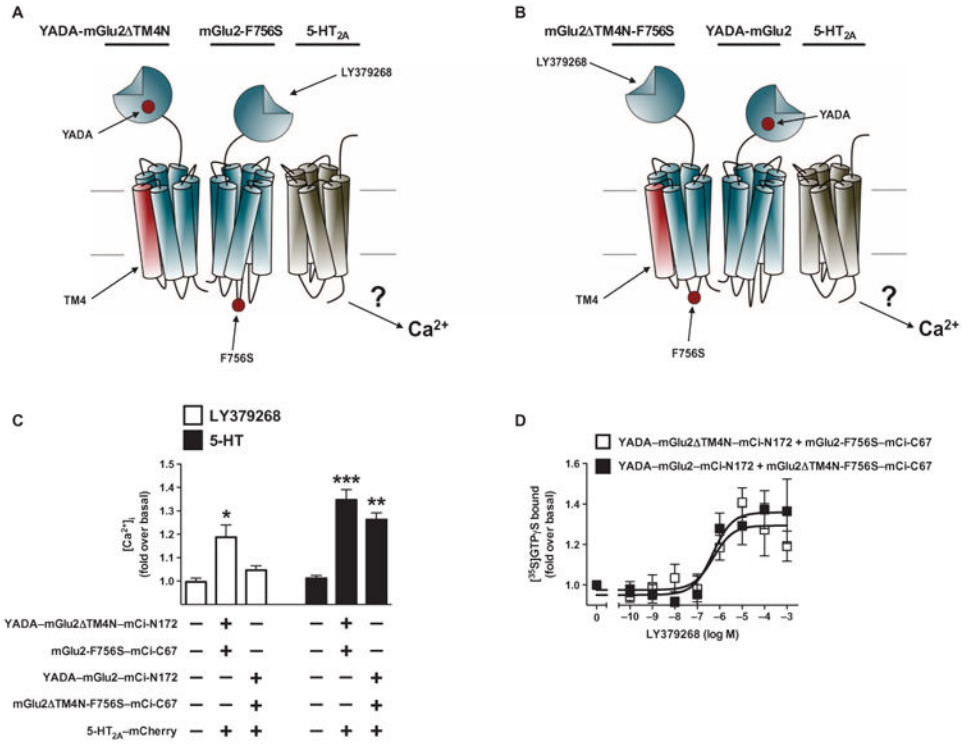

Fig. 3. The relative orientation of the two mGlu2 protomers affects 5-HT$_{2A}$ receptor–dependent G$_{q/11}$ coupling

(**A** and **B**) Cartoon representation of the relative positions of the components of the 5-HT$_{2A}$–mGlu2 heteromeric receptor complex that are necessary to induce Ca^{2+} release in the presence of the mGlu2/3 agonist LY379268 based on the mGlu2/mGlu3 chimeric and single point mutation constructs expressed in HEK 293 cells. (**C**) Measurement of Ca^{2+} release in HEK 293 cells that were left untransfected or were cotransfected with plasmids encoding the indicated constructs after sequential stimulation with LY379268 and 5-HT. Data are means ± SEM of three independent experiments. *$P < 0.05$, **$P < 0.01$, and ***$P < 0.001$ by Bonferroni's post hoc test of one-way ANOVA. (**D**) Measurement of LY379268-stimulated [^{35}S]GTPγS binding in plasma membrane preparations of HEK 293 cells coexpressing mCi-N172–and mCi-C67–tagged receptors. Data are means ± SEM of four to eight experiments, each performed in triplicate.

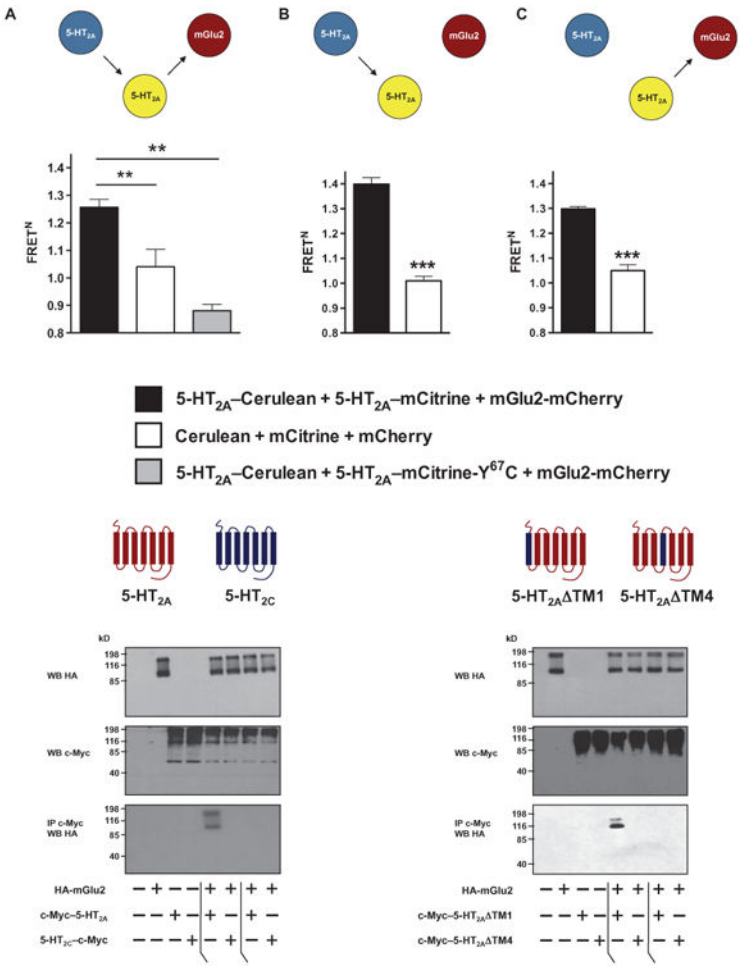

Fig. 4. Single-cell imaging and structure of oligomers of the 5-HT$_{2A}$–mGlu2 het-eromeric receptor complex

(**A** to **C**) Top: Cartoons illustrate the basis of direct and sequential FRET. Bottom: Three-color FRET (3-FRET) signals in cells expressing c-Myc–5-HT$_{2A}$–Cerulean, HA-mGlu2-mCherry, and either c-Myc–5-HT$_{2A}$–mCitrine or c-Myc–5-HT$_{2A}$–Y^{67}C-mCitrine. (A) Sequential 3-FRET was calculated by subtracting the signal in cells expressing Cerulean, mCitrine, and mCherry. Data are means ± SEM of 16 to 20 cells per group in three independent experiments. $^{**}P < 0.01$ by Bonferroni's post hoc test of one-way ANOVA. (B and C) Single FRET signals in cells expressing c-Myc–5-HT$_{2A}$–Cerulean/c-Myc–5-HT$_{2A}$–mCitrine and HA-mGlu2-mCherry. The single FRET signal from c-Myc–5-HT$_{2A}$–Cerulean/c-Myc–5-HT$_{2A}$–mCitrine (B) and the single FRET signal from c-Myc–5-HT$_{2A}$–mCitrine/HA-mGlu2-mCherry (C) were used to establish the appropriate conditions to measure both direct two-protein and sequential three-protein FRET. Data are means ± SEM of 16 to 20 cells per group in three independent experiments. $^{***}P < 0.001$ by Student's *t* test. (**D** and **E**) TM4 of 5-HT$_{2A}$ mediates complex formation with the mGlu2 receptor. Top: Schematic of the 5-HT$_{2A}$/5-HT$_{2C}$ chimeras studied. Bottom: HEK 293 cells coexpressing HA-mGlu2 and either c-Myc–5-HT$_{2A}$ or c-Myc–5-HT$_{2C}$ (D) or coexpressing HA-mGlu2 and either c-Myc–5-HT$_{2A}$ΔTM1 or c-Myc–5-HT$_{2A}$ΔTM4 (E) were subjected to coimmunoprecipitation (IP) with antibody against the c-Myc tag and then were analyzed by

Western blotting (WB) with anti-bodies against the indicated tags. As controls, HEK 293 cells separately expressing the c-Myc–or HA-tagged forms of the indicated receptors were mixed. Western blots are representative of three independent experiments.

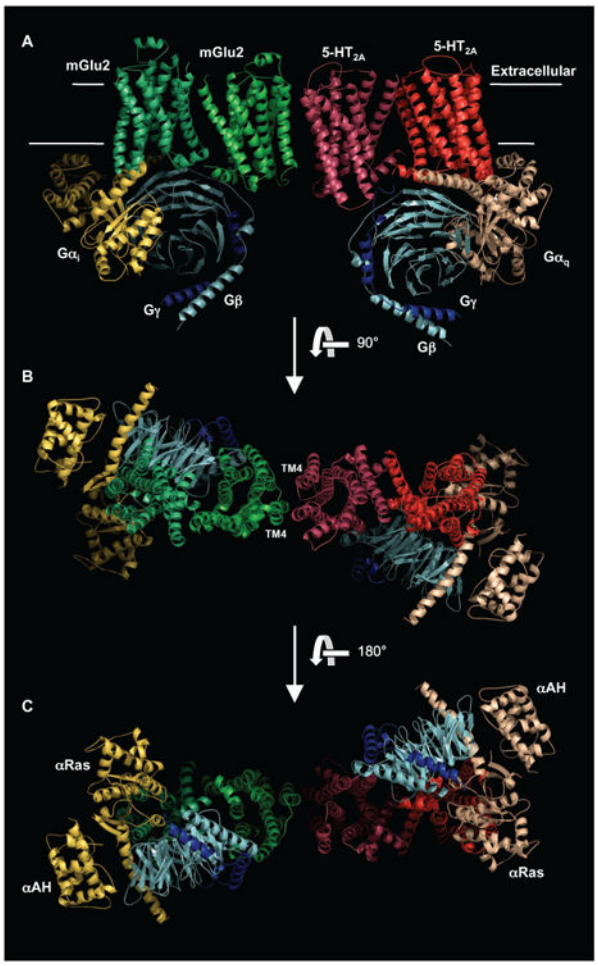

Fig. 5. Model for the docking of $G_{i/o}$ onto the 5-HT_{2A}–mGlu2 heteromeric receptor complex

(**A** to **C**) Ribbon representation of the vertical (A), extracellular (B), and cytoplasmic (C) views of the mechanism by which coupling of $G_{i/o}$ proteins to the mGlu2 protomer located distal to the 5-HT_{2A} component is necessary to enable allosteric crosstalk with 5-HT_{2A} and consequently activate $G_{q/11}$-dependent signaling. The homodimeric interfaces of mGlu2 and 5-HT_{2A} involve residues from TM1. The interface of the 5-HT_{2A}–mGlu2 heteromeric complex involves residues from TM4. αAH, α-helical domain of the Gα subunit; αRas, Ras-like domain of the Gα subunit.

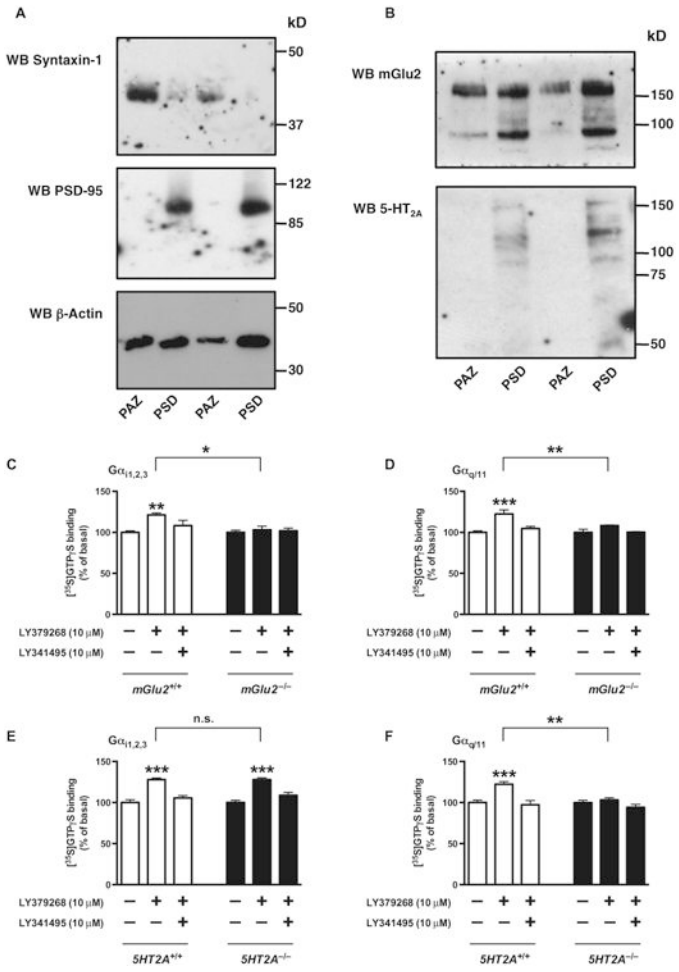

Fig. 6. Activation of $G_{q/11}$ by the mGlu2/3 agonist LY379268 is reduced in the frontal cortex of 5-HT_{2A} knockout mice

(**A** and **B**) Validation of the subcellular fractionation protocol performed to isolate PSDs and PAZs from the mouse frontal cortex. Equal amounts of proteins from mouse frontal cortex PSD and PAZ fractions were resolved by SDS-polyacrylamide gel electrophoresis (SDS-PAGE) and analyzed by Western blotting with antibodies against postsynaptic (PSD-95) and presynaptic (syntaxin-1) markers (A), as well as with antibodies specific for mGlu2 and 5-HT_{2A} (B). Western blots are representative of three independent experiments. (**C** and **D**) [^{35}S]GTPγS binding to frontal cortex membrane preparations of wild-type and mGlu2 knockout mice after treatment with vehicle or 10 μM LY379268 in the absence or presence of 10 μM LY341495 (the mGlu2/3 receptor antagonist) followed by immunopre-cipitation with anti-$G\alpha_{i1,2,3}$ (C) or anti-$G\alpha_{q/11}$ (D) antibodies. Data are means ± SEM of three or four independent experiments, performed in triplicate or quintuplicate for each condition. (**E** and **F**) [^{35}S] GTPγS binding to frontal cortex membrane preparations of wild-type and 5-HT_{2A} knockout mice after treatment with vehicle or 10 μM LY379268 in the absence or presence of 10 μM LY341495 followed by immunoprecipitation with anti-$G\alpha_{i1,2,3}$ (E) or anti-$G\alpha_{q/11}$ (F) antibodies. Data are means ± SEM of three or four independent experiments, performed in triplicate or quintuplicate for each condition. *$P < 0.05$, **$P < 0.01$, and ***$P < 0.001$ by Bonferroni's post hoc test of two-way ANOVA.

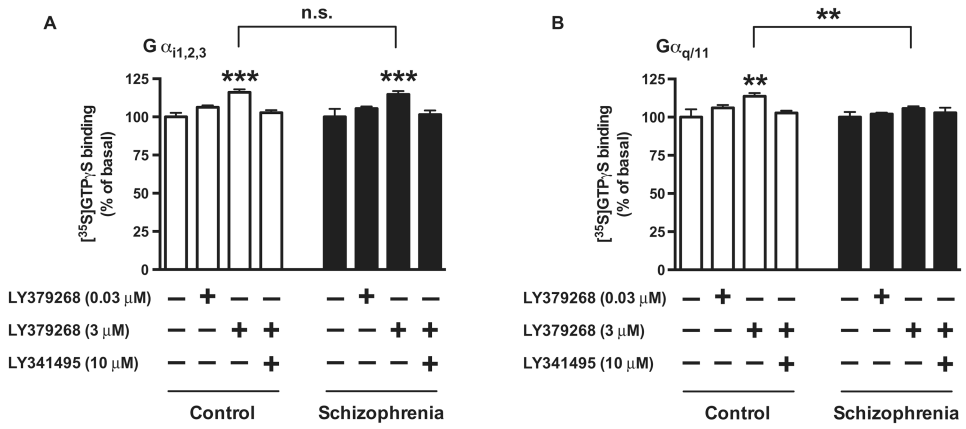

Fig. 7. Activation of $G_{q/11}$ by the mGlu2/3 agonist LY379268 is dysregulated in the postmortem brains of schizophrenic subjects

(**A** and **B**) [^{35}S]GTPγS binding in postmortem frontal cortexes of schizophrenic subjects and normal controls after treatment with vehicle or the indicated concentrations of LY379268 in the absence or presence of 10 μM LY341495 (the mGlu2/3 receptor antagonist) followed by immunoprecipitation with anti-$G\alpha_{i1,2,3}$ (A) or anti-$G\alpha_{q/11}$ (B) antibodies. Data are means ± SEM of 27 independent experiments, performed in triplicate or quintuplicate for each condition. See table S1 for demographic information and table S2 for pharmacological data. $^{**}P < 0.01$ and $^{***}P < 0.001$ by Bonferroni's post hoc test of two-way ANOVA.